A crude model to study radio frequency induced density modification close to launchers

Dirk Van Eester and Kristel Crombé

Citation: Physics of Plasmas **22**, 122505 (2015); doi: 10.1063/1.4936979
View online: http://dx.doi.org/10.1063/1.4936979
View Table of Contents: http://scitation.aip.org/content/aip/journal/pop/22/12?ver=pdfcov
Published by the AIP Publishing

A crude model to study radio frequency induced density modification close to launchers

Dirk Van Eester[1] and Kristel Crombé[1,2]
[1]*Laboratory for Plasma Physics (ERM/KMS), EUROfusion Consortium Member, Trilateral Euregio Cluster, Brussels, Belgium*
[2]*Department of Applied Physics, Ghent University, Ghent, Belgium*

(Received 10 April 2015; accepted 21 November 2015; published online 9 December 2015)

The interplay between radio frequency (RF) waves and the density is discussed by adopting the general framework of a 2-time-scale multi-fluid treatment, allowing to separate the dynamics on the RF time scale from that on the time scale on which macroscopic density and flows vary as a result of the presence of electromagnetic and/or electrostatic fields. The focus is on regions close to launchers where charge neutrality is incomplete and waves are commonly evanescent. The fast time scale dynamics influences the slow time scale behavior via quasilinear terms (the Ponderomotive force for the case of the equation of motion). Electrons and ions are treated on the same footing. Also, both fast and slow waves are retained in the wave description. Although this work is meant as a subtopic of a large study—the wave induced "convective cell" physics at hand is of a 2- or 3-dimensional nature while this paper limits itself to a single dimension—a few tentative examples are presented. [http://dx.doi.org/10.1063/1.4936979]

I. INTRODUCTION

The present paper discusses the interplay of radio frequency waves and plasma close to wave launchers. In this region, the temperature is sufficiently low for cold plasma wave models to be relevant but the density is so low that typically at least part of the wave power is carried by evanescent waves. The adopted model combines known ingredients but aims at providing a more complete description for wave induced density modification.

In view of the very different time scales involved in radio frequency (RF) wave physics, it makes sense to split the task of modeling the wave-plasma interaction into 2 subproblems: (i) one describing the fast time scale dynamics and in which the slow time scale variables can simply be assumed to be constant as a function of time and (ii) one describing the slow time scale dynamics, for which the fast dynamics only intervene through the second order corrections averaged over the relevant fast dynamics period or periods. All quantities are assumed to be the sum of a slowly varying term, topped up by a small, rapidly varying perturbation. This justifies linearizing the equations and obtaining a description for the deviations away from the slow time scale dynamics. Moreover, assuming transient behavior is of no concern, the fast time scale physics can be studied as a driven response to an oscillating drive at a prescribed wave frequency ω, i.e., $\partial/\partial t \rightarrow -i\omega$. When relevant, other fast time scale variations (in this particular case, the time dependence following from the Larmor gyrations the strong magnetic field imposes on the charged particles) equally need to be removed by a proper averaging when seeking to isolate the "pure" slow time scale response. Following this approach, the dynamics can be described by separate but coupled sets of equations, one set for each of the 2 individual time scales. The fast time scale description requires slow time scale quantities as input. The slow time scale description feels the influence of the fast time scale via quasilinear terms: Although the period-averaged perturbed quantities vanish, quadratic contributions do *not* and hence their time average adds a finite contribution to the slow time scale equations.

The linearization procedure standardly used when deriving wave equations for describing wave dynamics in tokamak plasmas relies on the fact that the static magnetic field by far exceeds the magnetic field of the externally launched waves. Along with the linearization of Maxwell's equations and the equation of motion to account for the strong impact of the confining field, it is customary to linearize the other equations describing the plasma. This is not without risk. In the context of the topic treated in the present paper, the linearization of the density is of specific concern: Whereas the density is high in the main plasma, this is not the case in the neighborhood of the antenna. Moreover—just because the density is low in that region—a dominant fraction of the wave power is carried by large amplitude evanescent waves. The density perturbation essentially being proportional to the square of the electric field magnitude, the wave induced density modification may not be small compared to the slow time scale density. When linearization fails, the here presented model loses its validity so an *a posteriori* check of the results is needed.

In a previous paper, the wave-induced density modification was computed assuming the electric field pattern is known.[1] Adopting a simple 2D wave model, the drift velocities setting up 2D convective cells were identified and the creation of a wave induced density asymmetry in front of the antenna was illustrated. In the present paper and unlike what was done before, the impact via the density modifications brought about *by* the waves *on* the waves themselves is accounted for by setting up an iterative scheme. Although it is clear that the dynamics of the convective cells cannot be captured fully in 1 dimension, the present paper restricts itself to slab geometry. The main reason is that a set of linear

and nonlinear equations needs to be solved simultaneously to get insight in the wave-particle dynamics. An intermediate step was judged to be necessary to examine if numerical stability for the relevant system of equations can be reached. The extension of this work to 2D or 3D is a logical and necessary step to be taken next.

Launchers are typically embedded in metallic boxes and excite waves close to metallic vessel walls. Close to such walls, charge neutrality is violated, and a potential difference between the wall and the deep plasma—where charge separation no longer exists—is set up. Adopting a given, simplified density profile, the interplay of the different kinds of waves supported by the plasma behind the last closed flux surface of a tokamak was studied by solving the cold plasma wave equation.[2] Although a fluid model lacks certain crucial ingredients to describe what happens very close to the wall, a somewhat more macroscopic description can be attempted adopting the here presented model. Metallic boundary conditions can be imposed for the RF waves but the wall voltage giving rise to charge separation is an input, not an output.

The present paper aims at offering a simple, consistent, first-principles framework for describing density modifications brought about by radio frequency waves, and at exploring this framework to describe the dynamics close to launchers in tokamak environment in the presence of both a strong confining magnetic field and RF power. Up to few exceptions, the ingredients used in this paper are "classical." The model that will be developed here is a (multi-)fluid model and hence—by definition—it excludes kinetic effects. In particular, it overlooks the fact that the velocity distribution function of the particles generally does not have a Gaussian shape at the modest densities close to the vessel walls and antennas, where the time spent by a particle in the modeled region is not enough to ensure collisional thermalization around a mean value. The often implicitly made assumption that particles sample a given location many times—as is the case for a particle on a closed magnetic surface in a tokamak—is not justified when modeling plasma behind the last closed flux surface. As a result, the routinely applied averaging that underlies the splitting of 2 time scales may become questionable for some applications. Moreover, quasilinear theory is applied, which—given the magnitude of the electric fields carrying MegaWatts of power into the tokamak—hinges on the assumption that the *net* effect of a rapid succession of events on a fast time scale can sensefully be captured by a slow time scale model in which the effect of the fast time scale shows up as a small, finite average over the oscillation period (or periods) of the fast time scale. It suffices to consult the work of Dirickx[3] on transport equations to realize that strong gradients necessitate the redevelopment of the whole drift ordering theory of the interaction of charged particles in the presence of electric and magnetic fields, a concept far beyond the more modest scope of the present paper.

The philosophy adopted in this paper is not new. In the context of high frequency lower hybrid waves (allowing to capture the wave dynamics by restricting the description to the parallel electric field component only) and implicitly assuming the density deviations are typically modest, Chan and Chiu discussed wave induced density depletion analytically already 3 decades ago for a number of relevant density models.[4] More recently, Meneghini relied on the 2-time scale separation to iteratively compute the wave induced density depletion close to the lower hybrid grill adopting the view that the various species obey a Boltzmann distribution.[5,6] Both of these works study wave dynamics in a frequency range where cross-talk between the various waves a cold plasma admits is absent. In the ion cyclotron frequency domain, wave-wave coupling is *routinely* occurring in the low density region close to the antenna and cannot be neglected. Moreover, even though the RF antenna is designed to launch fast waves, it also parasitically excites the slow wave in a magnetized plasma. A model describing both wave types and retaining all 3 wave components needs to be adopted when studying radio frequency waves.

The wave induced density depletion is interpreted to be due to the Ponderomotive force. Klima proposed an elegant way to compute this force.[7] It generalizes the expression adopted by Chan and Menegheni. As will be explained, both parallel and perpendicular electric field components have an impact, depending on which frequency range and which type of particles is studied.

Meneghini pointed out that an iterative technique for solving the relevant equations offers perspectives for applications in more than 1 dimension and he illustrated this by presenting 1D, 2D, and 3D results; his work aims at comparing reflectometer Alcator C-Mod density measurements with theoretical predictions. Going beyond a 1D description is also the longer term goal foreseen for the here presented work. There are a number of aspects that are not yet properly captured by the set of equations adopted in the present work which are thought to have a non-negligible bearing on the density profile that is set up: One is the fact that the large difference in mobility along and across magnetic field lines causes a sharp exponential decay of the density behind the last closed flux surface. The other is that ionization/recombination and sputtering modify the particle balance. Accounting for these processes is intended to be done when extending the here presented model to more than 1 dimension but for the time being the scope is limited to the usual framework also adopted in earlier work.

Furthermore, magnetic field lines are not necessarily fully parallel to the launcher, as is often assumed in tokamak wave modelling. Moreover, metallic structures might be intersecting field lines passing close to the antenna, and particles crudely following these field lines will undergo wave induced modifications. Recent theoretical as well as experimental works suggest that the effect of high power density waves can be observed well away from the antenna at places magnetically connected to it.[8,9] Finally, near metallic objects charge neutrality is violated, necessitating to account for the electrostatic potential set up by the charge imbalance. For that reason, the magnetic field is left arbitrary in this paper, and violation of charge neutrality is permitted.

An aspect that has, on purpose, been left out of the present description is the impact of kinetic corrections. Including kinetic effects makes the description more realistic but significantly more delicate and time consuming. As tackling the

global problem of wave-particle interaction in a complicated geometry is intractable with the present-day computers, one needs to make justified simplifications. While the philosophy of the adopted approach is the same (relying on linearization of the equations and on the quasilinear approach to describe the net impact of the fast time scale on the slow time scale), the bookkeeping becomes much more demanding (see, e.g., Refs. 10–12) and subtleties arise when going from fluid to kinetic descriptions, as is, e.g., documented in Ref. 13. Similar to what is done when deriving the equations governing the fluid description, kinetic models of the wave-particle cross-talk typically assume that the distribution function is only moderately deformed by the rapidly varying waves and one writes down a Fokker-Planck type equation for the slow time scale distribution function f_s, in which only the net effect of the rapidly varying terms is retained. Doing this in a sufficiently rigorous way while ensuring no artificial features show up is far from evident. Provided this first step has been taken successfully, taking moments results in fluid-type equations which then contain the effect of the RF waves as well as terms (e.g., pressure, stress, and collision terms) that are absent in single particle equations. A typical example is the work due to Hegna. Assuming f_s stays close to the Maxwellian, Hegna and Callen outlined a procedure to come up with such a practical set of upgraded fluid-type equations.[14]

It has been shown—e.g., by Devaux and Manfredi[15,16]—that kinetic corrections *do* matter when looking into the more detailed description of the wave-particle interaction. Devaux's kinetic computations show that the key deviations of the distribution function from the Maxwellian are that *zero order flows* need to be accounted for, i.e., that f_s is no longer centered around $\vec{v} = \vec{0}$. In a somewhat crude way, the notion of temperature linked to the spread of the distribution around the average flow velocity $\vec{v}_o$ in velocity space survives in a fluid model, be it that kinetic computations show that *deformations* away from a Gaussian spread around $\vec{v}_o$ are usually observed. Prior to tackling the problem fully kinetically, the results of Devaux indicate, however, that one might make progress in understanding the wave-particle cross-talk in steps, one step consisting in retaining the flows but still sticking to a multi-fluid description which is relatively modest in required computational power, and the other adding the kinetics responsible for the velocity space deformations away from a Gaussian spreading about the mean flow. It should be noted that the presence of zero order flows strictly requires that the cold plasma dielectric tensor—which has been derived assuming $\vec{v}_o = \vec{0}$—should be upgraded as well. Sufficiently general kinetic models (see, e.g., Refs. 17–19) automatically incorporate both the macroscopic flow and the deviations of the distribution away from it, but rigorously solving the wave-particle interaction problem involving high frequency waves that significantly modify the distribution is, at this moment, a challenging task for addressing hot core dynamics (see, e.g., Ref. 20). And it is an even bigger challenge in low temperature, low density regions in which the assumptions underlying kinetic treatments are poorly justified. Awaiting further theoretical development and for physics aspects that require including kinetic effects, at present, the only available alternative is brute force modeling maximally tapping into the potential of the presently available computing power. Over the last years, numerical modeling of tokamak plasmas has increasingly more relied on supercomputers (for examples on waves in the tokamak edge see, e.g., Refs. 21 and 22). For example, Monte-Carlo/PIC (particle-in-cell) modeling does exactly that. This technique attempts to treat the plasma the way it is: as a large number of individual particles interacting with each other. It has the advantage that physics processes can be included fairly easily and that there is no need for linearization or splitting timescales. The downside is that the full complexity of a tokamak plasma is statistically ill grasped. For problems that take place in a very small physical volume and where a stationary state is reached after tracking the evolution for a limited number of cycles of the fast time scale, this technique offers a great potential.[22] But when needing to track particles for longer distances over bigger volumes (experimental evidence shows that the influence of wave power is felt meters away from launchers[9]), ensuring that a sufficient number of particles is traced to make the description statistically relevant soon becomes an unsurmountable challenge, in spite of the already huge possibilities offered by parallel processing.

In view of its many weaknesses, one may wonder if it makes sense to even attempt to adopt the framework of a fluid theory and the quasilinear approximation to capture near-field physics. The authors' approach is pragmatical: In view of the lack of a fully developed theory incorporating steep gradients, kinetic effects, and an integro-differential description of the dielectric response in a full 3D geometry, it seems worthwhile to assess the potential of a *simplified* theory to at least present a qualitative, consistent picture of the dynamics that can be used to help understand experimental findings. Lacking certain ingredients (the multidimensional nature of the physics and the inclusion of transport being trivial ones), it is clear that quantitative agreement cannot be hoped for and requires further work. On the other hand, the model presented here combines many of the contributions identified as important in the literature in various limits and does so yielding a model that is not overly CPU time consuming.

This paper is structured as follows: First, the relevant set of equations is sketched and/or derived. Different subsections are devoted to the various equations. In Section III, the actual 1D version of the adopted set of equations is given. Also, the adopted method to solve the obtained mixed set of linear and non-linear equations is discussed. In Section IV, some practical examples are given. Finally, conclusions are drawn and a brief discussion sketches the way ahead.

II. THE RELEVANT SET OF EQUATIONS

To model the interplay of a plasma and electromagnetic waves, adopting 3 types of equations is a bare minimum:

- Solving Maxwell's equations yields the electromagnetic field pattern arising for a given current density.
- Solving the equation of motion learns how the plasma momentum for each type of species is modified under the

influence of the relevant forces, the Lorentz force, in particular.
- Solving the continuity equation provides the density consistent with the flows resulting from the equation of motion for each population.

In the present paper, it is assumed that the temperature T is constant. In the region close to the launcher, T is typically a few to a few tens of eV. The above set needs to be supplemented with an energy evolution equation in case more detailed knowledge of the temperature is required.

A. Equation of motion

Klima derived expressions for the slow scale equation of motion for charged particles in the presence of a confining magnetic field and when a driven high frequency electromagnetic field perturbs the motion.[7] The relevant equation was first derived for particles and was then generalized for a gas of identical charged particles. Klima introduces an ordering that separates the fast and slow time scales and explicitly assumes that they are well separated so that the relative magnitude of their characteristic time scales t_{fast}/t_{slow} defines a small parameter δ. The slow time scale equations describe the motion smoothed with respect to the fast dynamics and are accurate up to δ^2; higher order corrections are systematically dropped. In the present paper, Klima's equation of motion will be adopted. For the Ponderomotive term, a similar derivation was recently obtained.[1] The expression due to Klima is an average over the driver period and relies on the fast time scale motion being purely driven but retains the effects of the fast time scale magnetic field. The latter expression integrates the actual equation of motion on the fast and slow time scale assuming the magnetic field is constant while ignoring the impact of the perturbed magnetic field on the motion and represents an average over the driver as well as cyclotron period. Although numerically indistinguishable in the homogeneous plasma limit for RF applications, Klima's expression is preferred here because it includes the full perturbed Lorentz force and yields a more symmetrical expression, which is more suitable for analytical integration.

The starting point is the single particle equation of motion under the influence of the Lorentz force. Since the Lorentz force due to the strong, static magnetic field dominantly imposes the orbit of the charged particles while the RF field adds a small but rapidly varying perturbing force to it, the equation of motion is linearized. Splitting the position and the velocity into a slow and a small but rapidly varying contribution ($\vec{x} = \vec{x}_o + \vec{\rho}_1$, $\vec{v} = \vec{v}_o + \vec{v}_1$) and neglecting higher than first order corrections of the fields, the slow flow is captured by solving the equation

$$m\frac{d\vec{v}_o}{dt} = q\vec{E}_o + q\left[\vec{v}_o \times \vec{B}_o + \left\langle \frac{d\vec{\rho}_\Omega}{dt} \times (\vec{\rho}_\Omega.\nabla)\vec{B}_o \right\rangle\right] + \vec{F}_{RF}, \tag{1}$$

in which $\vec{F}_{RF}$ is the net force due to the rapidly varying aspects of the driven motion, i.e.,

$$\vec{F}_{RF} = \left\langle q\left[\vec{v}_1.\nabla\vec{E}_1 + \vec{v}_1 \times \vec{B}_1 + \frac{d\vec{\rho}_1}{dt} \times (\vec{\rho}_1.\nabla)\vec{B}_o\right]\right\rangle, \tag{2}$$

and where $\langle \ldots \rangle$ denotes the smoothing time average; for convenience, the cyclotron and driven motions are split into the cyclotron rotation part (denoted with a subscript "Ω") and a driven part. By definition, the driven oscillation (denoted with the subscript "1") satisfies

$$\begin{aligned} \vec{v}_1 &= -i\omega\vec{\rho}_1 \\ -i\omega m\vec{v}_1 &= q[\vec{E}_1 + \vec{v}_1 \times \vec{B}_o], \end{aligned} \tag{3}$$

in which ω is the driver frequency and a driven response $\propto \exp[-i\omega t]$ was assumed. $\vec{B}_o$ and $\vec{E}_o$ are the static magnetic and electric fields, respectively. The $\vec{F}_{RF}$ term is known as the Ponderomotive force (see, e.g., Ref. 23 for the more commonly known derivation in the absence of a magnetic field). Assuming the static magnetic field gradient is large but its gradient negligibly small, and adopting complex notation so that the time average of a quadratic driven quantity over a period is $\langle AB \rangle = Re[A^*B]/2$, the corresponding acceleration can be written as

$$\vec{a}_{Pond} = -\nabla\Theta, \tag{4}$$

where

$$\begin{aligned} \Theta &= \frac{1}{4}\left[\frac{1}{\omega^2 - \Omega^2}\right]\left[|\vec{\epsilon}|^2 - \left|\frac{\vec{\epsilon}.\vec{\Omega}}{\omega}\right|^2 + \frac{i}{\omega}\vec{\Omega}.\vec{\epsilon}^* \times \vec{\epsilon}\right] \\ &= \frac{1}{4}\left[\frac{1}{\omega^2 - \Omega^2}\right]\left[|\vec{\epsilon}|^2 - \left|\frac{\vec{\epsilon}.\vec{\Omega}}{\omega}\right|^2 - \frac{2\Omega}{\omega}Im\left[\epsilon^*_{\perp 1}\epsilon_{\perp,2}\right]\right], \end{aligned} \tag{5}$$

in which $\vec{\Omega} = q\vec{B}_o/m$ and where Faraday's law was used to eliminate the perturbed magnetic field $\vec{B}_1$ in favour of the perturbed electric field $\vec{E}_1$; the notation $\vec{\epsilon} = q\vec{E}_1/m$ was introduced.

Subsequently, Klima extends the result found for single particles to the case of a flow adopting the assumption that the pressure is of order δ^2. Assuming the temperature T is constant, the generalized equation of motion

$$\frac{d\vec{v}_o}{dt} = -v_t^2\frac{\nabla N_o}{N_o} - \frac{q\nabla\Phi}{m} - \nabla\Theta + \Omega\vec{v}_o \times \vec{e}_{//} \tag{6}$$

is obtained. Here, N_o is the density and $v_t^2 = kT/m$ is the square of the thermal velocity. Some details of the derivation can be found in Appendix A. The linearization of the equation of motion being based on the fact that the confining magnetic field is strong, the relative magnitude of the various terms in the static acceleration $\vec{a}$ is not bound to restrictions. However, the adopted ordering needs to be justified *a posteriori*, and focusing on certain aspects might require a more refined model. Solving the relevant equation of motion Eq. (6) can be done as an initial value problem (in which case not only the equation for the velocity but also that for the position needs to be solved) or as a boundary value problem (in which case the time derivative is local and the solution is convected by the convection term). Two examples are discussed in Appendix B.

For a *given* static acceleration $\vec{a} = -v_t^2/N_o \nabla N_o - q\nabla\Phi/m - \nabla\Theta$, the perpendicular part of Klima's equation of motion can be integrated by hand. One gets

$$\begin{aligned} v_+ &= v_{+0}\exp[-i\Omega t] + \frac{a_+}{i\Omega}, \\ v_- &= v_{-0}\exp[+i\Omega t] + \frac{a_-}{-i\Omega}, \end{aligned} \tag{7}$$

(where $v_\pm = v_{\perp,1} \pm i v_{\perp,2}$) which consists of a rapidly varying contribution oscillating at the cyclotron frequency, and a slow drift term *across* the magnetic field lines of the usual form

$$\begin{aligned} \vec{v}_{drift,\perp} &= \frac{1}{qB_o^2}\vec{F}\times\vec{B}_o = \frac{1}{\Omega}\left[\vec{a}\times\vec{e}_{//}\right] \\ &= \frac{1}{\Omega}[\vec{e}_{\perp,1}a_{\perp,2} - \vec{e}_{\perp,2}a_{\perp,1}]. \end{aligned} \tag{8}$$

Aside from the $\vec{E}_o \times \vec{B}_o$ drift due to the electrostatic field $\vec{E}_o = -\nabla\Phi$ and the diamagnetic drift due to the $\nabla P = kT\nabla N_o$ force, the above equation consists of a Ponderomotive contribution due to the finite RF electric field. This solution is found by first integrating the equation in the absence of $\vec{a}$ and assuming $\vec{B}_o$ to be constant, and then by relying on the technique of the variation of constants to introduce the effect of the finite $\vec{a}$. In the latter, the effect of a slightly inhomogeneous magnetic field could be introduced *a posteriori* by a supplementary $m/[qB_o^3][v_{//}^2 + v_\perp^2/2]\vec{B}_o \times \nabla B_o$ velocity drift term. On the relevant scale length, the changes of $\vec{B}_o$ in the antenna region of a tokamak are modest both in amplitude and direction. Note that the obtained perpendicular drift satisfies $d\vec{v}_{o,\perp}/dt = \vec{0}$ in an elegant way: it is time independent (hence $\partial\vec{v}_o/\partial t = 0$) and it is homogeneous (hence $\nabla\vec{v}_o = 0$ and thus $\vec{v}_o.\nabla\vec{v}_o = 0$). As a result, the simplified equation

$$\vec{a} + \vec{v}_o \times \vec{B}_o = 0 \tag{9}$$

is satisfied by the driver-period and cyclotron-period averaged slow time scale velocity.

Klima isolates 2 types of motion (the driven motion and the slow time scale motion) but does not actually solve the equations and hence does not remove the fast cyclotron oscillation forced by the Lorentz term in case B_o is strong. This can easily be done by isolating the drift velocity from the cyclotron oscillation in Eq. (7) by performing a gyro-average, which eliminates the fast terms. From this point in the paper onwards $\vec{v}_o$ will represent the zero order velocity averaged both over the driven *and* cyclotron motions. As demonstrated earlier, this yields the steady state equation Eq. (9) —providing $\vec{v}_{o,\perp}$—to be satisfied in the perpendicular direction and the parallel equation of motion to be solved numerically to identify $v_{//}$ for a prescribed $\vec{v}_{o,\perp}$ (see further). Note that the perpendicular drift is divergence-free provided Ω is constant, and that it conserves the perpendicular energy ($\vec{a}_\perp.\vec{v}_{drift,\perp} = 0$), i.e., it is a force-free flow.

A key point to the approach adopted is that Eq. (6) is solved *by hand* fully including the time dependence upon considering the forces aside from the Lorentz force due to the confining magnetic field to be *static*. The Lorentz force term explicitly contains the velocity $\vec{v}_o$ and hence cannot offhand be considered to be time-independent.

The fact that the acceleration $\vec{a}$ is static does not mean that its effect is small: The gradient of the density can be steep and hence the drift perpendicular to the magnetic field and—depending on the $\vec{B}_o$ orientation—parallel and/or perpendicular to the metallic wall can be significant. On top of that, the equation for the parallel motion is nonlinear. As will be discussed later in this paper, the burden of finding the correct solution to the equation is put on the computer. Rather than solving the non-linear equations directly, an iterative scheme is introduced. The desired solution is the asymptotic solution of an iteration scheme; at each iteration, a set of linear equations is solved. A similar approach was used by Louche[24] when solving the Fokker-Planck equation for the RF heated *majority*, necessitating the use of the nonlinear collision operator and a similar approach was proposed by Meneghini[5,6] when studying wave induced density modification in front of a Lower Hybrid grill. Because drifts perpendicular to reigning gradients are created due to the presence of the strong confining magnetic field, the dynamics *cannot* fully be captured adopting a 1D model and the description in this paper is necessarily incomplete.

The fast time scale effect was removed from the perpendicular dynamics by averaging over the cyclotron period, which yields a net drift. The magnetic field is incapable of accelerating particles along its field lines. Opposite to what was needed for the perpendicular motion, omitting the slow time variation altogether ($\partial/\partial t \rightarrow 0$) is reasonable straightaway. Assuming that the confining magnetic field is strong so that the perpendicular drift velocity is modest—allowing it to be neglected as a first approximation ($\vec{v}_o.\nabla \approx v_{//}\partial/\partial x_{//}$; this approximation will be relaxed a few lines further)—the equation of motion for the parallel motion can be written as

$$v_{//}\frac{\partial}{\partial x_{//}}v_{//} = -v_t^2\frac{\partial lnN_o}{\partial x_{//}} - \frac{q}{m}\frac{\partial\Phi}{\partial x_{//}} - \frac{\partial\Theta}{\partial x_{//}} \tag{10}$$

which can be integrated analytically to yield

$$N_o = N_{o,ref}\exp\left[-\frac{1}{v_t^2}\left(\frac{v_{//}^2}{2} + \frac{q\Phi}{m} + \Theta\right)\right]. \tag{11}$$

The above is a generalisation of the Boltzmann expression incorporating the impact of the parallel flow and of the RF Ponderomotive force aside the usual electrostatic potential. The terms $v_{//}^2/2$, $q\Phi/m$, and Θ play a similar role in the density variation and are all position-dependent. For a simple plane wave solution, $\vec{E} \propto \exp[ik_x x]$, the density change caused by the electric field scales as the derivative of Θ: $dlnN_o/dx|_{RF} = 2Im[k_x]\Theta/v_t^2$. This readily shows that the effect of the waves on the density is much more pronounced when waves are *evanescent* than when waves are propagative. Furthermore, as $\Theta \propto |\vec{\epsilon}|^2$ the density modification scales with the square of the electric field. For both of these reasons, wave-induced density depletion is expected to be much stronger close to wave launchers than away from

them. Moreover, short wavelength branches have a stronger impact than long wavelength modes.

Studying plasma dynamics close to metallic surfaces, it is routinely assumed that electrons satisfy the Boltzmann expression $N_e = N_{e,ref}\exp[e\phi/kT]$ in which $N_{e,ref}$ is the reference density at the location where the potential ϕ is zero. For a thermalized plasma close to a metallic wall, the differing mass and thus mobility of ions and electrons cause electrons to load the wall negatively ($\phi_{wall} < 0$), after which it repels electrons; $|\phi_{wall}|$ is typically about $3kT/e$ (see, e.g., Ref. 25). The Boltmann expression describes the ensuing density depletion close to the wall. When an oscillating voltage is imposed on the wall, the potential ϕ in this expression responds to the wall voltage and is the sum of an electrostatic Φ and a driven, rapidly varying part $\Phi_{RF}cos\omega t$ (see, e.g., Ref. 26): $\phi = \Phi + \Phi_{RF}\cos\omega t$. The mean value of the density averaged over a period T_{RF} of the driver can be computed to be[27]

$$\frac{1}{T_{RF}}\int_0^{T_{RF}} N_{ref}\exp\left[\frac{e\phi}{kT}\right]dt = N_{ref}\exp\left[\frac{e\Phi}{kT}\right]I_0\left(\frac{e\Phi_{RF}}{kT}\right). \quad (12)$$

If the RF potential is very small, then the average density scales as $\propto exp[e\Phi/kT]$. If it is large then the main scaling becomes $\propto exp[e(\Phi+\Phi_{RF})/kT]$. The density response to the electrostatic Φ and the Ponderomotive potential $\Phi_{Pond} = m\Theta/q$ described in Eq. (11) is seen to play a similar role as the sheath potential and the RF potential, respectively. Rather than being externally driven, the metallic wall will now respond to the presence of the RF waves bouncing off it. These waves need not be electrostatic in nature.

It is instructive to evaluate the Ponderomotive potential Φ_{Pond} for a typical case to get a sense of the magnitude of the term; recall that the electrostatic potential is typically of the order of a few times the electron temperature. In the ion cyclotron region of frequencies, the electron cyclotron frequency is much larger than that of the driver frequency. Hence for electrons,

$$\Phi_{Pond,e} = -\frac{m_e\Theta_e}{e} \approx -1.11\times10^{-3}\left|\frac{E_{//}[\mathrm{V/m}]}{f[\mathrm{MHz}]}\right|^2.$$

For ions one gets

$$\Phi_{Pond,i} = \frac{m_i\Theta_i}{q_i} \approx 6.07\times10^{-7}\frac{Z_i}{\tilde{\alpha}A_i}\left|\frac{E[\mathrm{V/m}]}{f[\mathrm{MHz}]}\right|^2,$$

in which the factor $\tilde{\alpha}$ is of order 1; it accounts for the difference in magnitude between Ω and ω and for the polarization. Electrons thus are primarily influenced by the *parallel* electric field while the ions feel the influence of the total field. In the expression of the density, these terms appear as $\Theta/v_t^2 = (q/kT)\Phi_{Pond}$. In JET (Joint European Torus), the A2 antenna is at major radius $R_{ant} = 3.9$ m in the equatorial plane. Central hydrogen minority heating in a deuterium plasma—the most commonly adopted ICRH (ion cyclotron resonance heating) heating scheme in JET—is typically done at $B_o = 3.45$ T in the plasma core and adopting $f = 51$ MHz. Neglecting the effect of the poloidal magnetic field, this yields a magnetic field strength of 2.62 T at the antenna location and hence $\Omega_D = 1.25\times10^8$ rad/s and $\Omega_e = -4.61\times10^{11}$ rad/s. For the majority ions, $\Omega/\omega \approx 0.4$ while for the electrons ω can be neglected w.r.t. Ω. Consider an edge temperature of $T_e = T_i = 5$ eV. For the electrons the density e-folding requires $E_{//} \approx 3.4$ keV/m. Figure 1 depicts the variation of the density along a magnetic field line as a result of the variation of the parallel velocity or of the potential for a deuterium plasma. As the electrostatic potential Φ and the Ponderomotive potential $m\Theta/q$ play a similar role, only Φ was varied. Anticipating the fact that both the electron and ion flow velocity are of the order of the sound velocity $c_s = (\gamma Z_i kT/m_i)^{1/2}$ (Bohm criterium; for a mono-atomic gas $\gamma = 1.4$–1.6), the parallel velocities are expressed in terms of c_s in the figure. Because the electron thermal velocity is much larger than that of the ion sound velocity, the electron density is hardly modified by changes of the parallel velocity. As the differing electron and ion mobilities cause the wall to charge negatively, the potential has been scanned only for negative values. Potential dips of up to $20\,V$ (simple models show the sheath voltage is of order $3kT_e/e$; in other regions where the charge separation is less pronounced the voltage drop is smaller) cause the electron density depletion to be almost complete. Due to the dependence on the charge, the ion density potentially *increases* and does so by up to a factor 50 for fixed $v_{//}$. An increase of the parallel velocity significantly moderates this ion density increase. As will be shown later when solving all relevant equations simultaneously, the variation of the parallel velocity and that of the density are intimately coupled. Hence, the here depicted variation only indicates the trend and cannot not be used as a prediction for the actual density change. For the Ponderomotive potential to be as important as the electrostatic potential in the exponent of the expression for the density

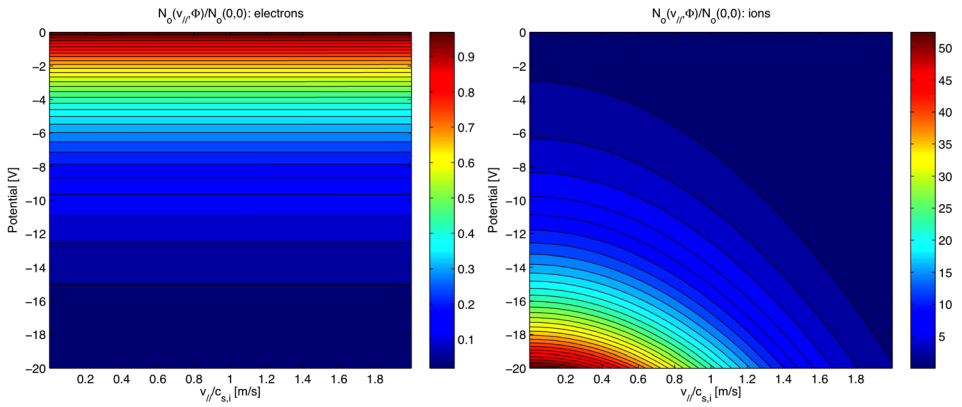

FIG. 1. Electron and (majority) ion density modification along magnetic field lines as a result of a $v_{//}$ or potential change.

requires $|E_{//}| \approx 5\text{kV/m}$ for the electrons and $|E| \approx 300\,\text{kV/m}$ for the ions; a reference value $\Phi = 10\,V$ was used to obtain these values. Such values are perfectly feasible close to the launcher, and in particular, inside the antenna box of multi-MegaWatt launchers where voltages of tens of kV are applied on straps that are only centimeters away from grounded metallic antenna boxes, but—depending on the local $\vec{B}_o$ direction—they may not be representative (much too large) very close to metallic surfaces. Remind, however, that it is not the actual value of Θ or Φ_{Pond} but its *gradient* that is important in the force balance. Constant amplitude propagative waves do not give rise to density modification. Steep gradients can occur and necessitate taking a closer look at the interplay of the various effects.

In general, the magnetic field is not strong enough for the drift terms in the parallel equation of motion to be neglected altogether. If the upgraded Boltzmann expression cannot be exploited, the change of $v_{//}$ is then described by

$$v_{//}\frac{\partial}{\partial x_{//}}v_{//} = -\left[\vec{v}_{drift,\perp}.\nabla v_{//} + v_t^2\frac{\partial lnN_o}{\partial x_{//}} + \frac{q}{m}\frac{\partial \Phi}{\partial x_{//}} + \frac{\partial \Theta}{\partial x_{//}}\right], \tag{13}$$

which can no longer be integrated analytically.

B. Fast time scale wave equation

For a given density, the fast time scale wave equation can be solved. It is implicitly assumed here that the static magnetic field is constant. $\vec{B}_o$ can point in any direction, though, so field lines can intersect the launcher and the nearby metallic walls. Two relevant Cartesian coordinate frames $(x_{\perp,1}, x_{\perp,2}, x_{//})$ and (x, y, z) are connected by 2 consecutive rotations (see Fig. 2). First keeping the z-axis fixed rotating over the angle α and then freezing the new y-axis and rotating over β to align the final z'' axis with $\vec{B}_o$ yields

$$\begin{pmatrix}\vec{e}_{\perp,1}\\ \vec{e}_{\perp,2}\\ \vec{e}_{//}\end{pmatrix} = \begin{pmatrix}\cos\beta\cos\alpha & \cos\beta\sin\alpha & -\sin\beta\\ -\sin\alpha & \cos\alpha & 0\\ \sin\beta\cos\alpha & \sin\beta\sin\alpha & \cos\beta\end{pmatrix}.\begin{pmatrix}\vec{e}_x\\ \vec{e}_y\\ \vec{e}_z\end{pmatrix} = \bar{\bar{\mathcal{R}}}.\begin{pmatrix}\vec{e}_x\\ \vec{e}_y\\ \vec{e}_z\end{pmatrix}. \tag{14}$$

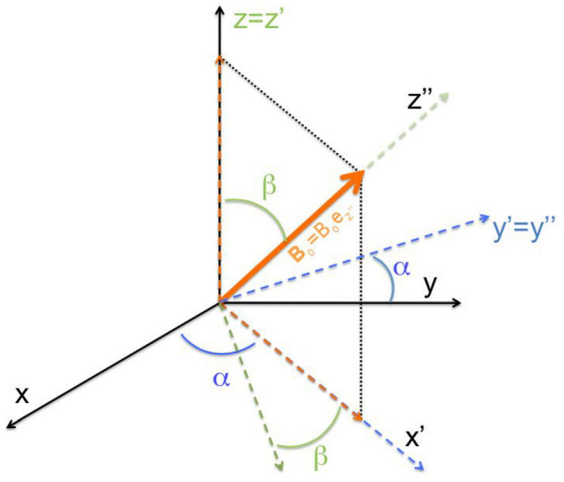

FIG. 2. Sheath (x, y, z) and magnetic field (x'', y'', z'') based coordinate frames.

In this paper, the dielectric response is modeled relying on the usual cold plasma dielectric tensor (see, e.g., Refs. 23 and 28). This choice—which ignores the presence of zero order flows $\vec{v}_o$ when relating the driven velocity and the driving field—is dictated by the wish to keep the model as simple as possible. But since flows are an integral part of wave induced density modification, this choice needs to reviewed at some point in the future. The immediate consequence is that the fast time scale equation of motion needs to be solved in parallel with Maxwell's equations and the dielectric response needs to be described via the current density, i.e., no general purpose dielectric tensor relating fast time scale velocities and electric fields can be provided here. Up to a differing choice of the angles α and β, the specific implementation of the relevant wave equation for finite $\vec{v}_o$ was already commented on in Ref. 1. For homogeneous plasmas and when the perturbations can be described by a single Fourier mode, upgrading the model amounts to extra Doppler shift terms $\vec{k}.\vec{v}_o$ in the analytically invertible equation of motion linking the perturbed velocity to the RF electric field. For inhomogeneous plasmas also gradients of the zero order flow velocity appear in the equation of motion. Except in particular cases, the inversion is non-trivial and a simple link between the velocity and the electric field no longer exists, i.e., the concept of a dielectric tensor that can be written in explicit form needs to be abandoned.

Assuming the variations in the x-direction dominate the variations in the 2 independent directions tangent to the wall, the y- and z-directions can be assumed ignorable for the zero order quantities and the variation of the rapidly varying electric field can be described by a double sum of *decoupled* Fourier modes (k_y, k_z). In terms of each (k_y, k_z), the wave equation can be written as

$$\left[\begin{pmatrix}k_y^2+k_z^2 & 0 & 0\\ 0 & k_z^2 & -k_yk_z\\ 0 & -k_yk_z & k_y^2\end{pmatrix} + \begin{pmatrix}0 & ik_y & ik_z\\ ik_y & 0 & 0\\ ik_z & 0 & 0\end{pmatrix}\frac{d}{dx} + \begin{pmatrix}0 & 0 & 0\\ 0 & -1 & 0\\ 0 & 0 & -1\end{pmatrix}\frac{d^2}{dx^2}\right]\begin{pmatrix}E_x\\ E_y\\ E_z\end{pmatrix} = k_0^2\bar{\bar{\mathcal{R}}}^{-1}.\bar{\bar{K}}_{NR}.\bar{\bar{\mathcal{R}}}, \tag{15}$$

in which $\bar{\bar{\mathcal{R}}}$ is the above defined rotation matrix (see Eq. (14)), $\bar{\bar{K}}_{NR}$ is the usual non-rotated cold plasma dielectric tensor with respect to the $\vec{B}_o$-based directions $(\vec{e}_{\perp,1}, \vec{e}_{\perp,2}, \vec{e}_{//})$, and $k_o = \omega/c$ where ω is the driver frequency and c the speed of light. Since the cold plasma dielectric tensor is a *matrix* rather than a differential operator, the above equation can immediately be generalized to 2 or 3 dimensions by substituting $(k_y, k_z) \rightarrow -i(d/dy, d/dz)$. Only when finite temperature corrections or inhomogeneity or drift effects are accounted for gradient terms appear in the dielectric response while here $\vec{B}_o$ is assumed constant both in amplitude and direction. In this exploratory paper, the description is limited to a single dimension.

As E_x is a linear combination of the other 2 wave components and their first derivatives for each (k_y, k_z), it can be

eliminated when solving the system. As $\bar{\bar{\mathcal{R}}}^{-1} = \bar{\bar{\mathcal{R}}}^{T}$, it is readily observed that the unit vectors along the coordinate lines transform as the corresponding vector components. Note that describing the variations along the magnetic field requires the differential operator

$$\vec{e}_{//}.\nabla = \frac{\partial}{\partial x_{//}} = \mathcal{R}_{31}\frac{d}{dx} + i\mathcal{R}_{32}k_y + i\mathcal{R}_{33}k_z$$
$$= \cos\alpha\sin\beta\frac{d}{dx} + i\sin\alpha\sin\beta k_y + i\cos\beta k_z.$$

Consequently, the parallel wave number is not a constant in general. As a result, the dispersion equation cannot be evaluated in the usual way by first solving for a prescribed $k_{//}$ to get the perpendicular wave numbers $k_\perp^2$, from which subsequently the k_x values can be found. Only when $\alpha = \pi/2$ or $\beta = 0$, the parallel wave number is a constant. Assuming the waves are decoupled at the plasma interface, the cold plasma dispersion equation—found by substituting $d/dx \to ik_x$ in the above wave equation and seeking for nontrivial solutions by imposing the system determinant is zero—can be solved and the 4 possible kinds of waves (2 of the fast wave and 2 of the slow wave type) are identified. Rather than appearing as pairs $(k_x, -k_x)$ corresponding to a common k_x^2 for a prescribed $k_{//}$, the 4 roots of the dispersion equation are typically distinct.

Four boundary conditions are required to uniquely define the solutions of this fourth order differential equation. The boundary conditions at the metallic wall are $E_y = E_z = 0$. The other 2 boundary conditions are imposed at the interface x_p of the region of interest with the deeper plasma. Assuming the various modes supported by the plasma are decoupled at the plasma interface, solving the polarization equation for each of the wave types yields the eigenvectors. The independent variables and the eigenvectors $\vec{s}_i$ are related by the matrix $\bar{\bar{T}}$

$$\begin{pmatrix} E_y \\ dE_y/dx \\ E_z \\ dE_z/dx \end{pmatrix} = \bar{\bar{T}}.\begin{pmatrix} s_1 \\ s_2 \\ s_3 \\ s_4 \end{pmatrix}$$
$$= \begin{pmatrix} a_1 & a_2 & \dots \\ a_1 ik_{x,1} & a_2 ik_{x,2} & \dots \\ a_1 E_z/E_y|_1 & a_2 E_z/E_y|_2 & \dots \\ a_1 ik_{x,1} E_z/E_y|_1 & a_2 ik_{x,2} E_z/E_y|_2 & \dots \end{pmatrix}.\begin{pmatrix} s_1 \\ s_2 \\ s_3 \\ s_4 \end{pmatrix}. \quad (16)$$

The coefficients a_i are guaranteeing that the electric field components of each of the reference eigenvectors corresponding to the roots $k_{x,i}$ have unity amplitude. At any location, the full electric field is a combination of fast (FW) and slow waves (SW). Referring to the various eigenvectors, a natural choice for the boundary conditions is to impose that only 1 kind of wave carries energy into the region of interest. This then, e.g., requires $s_{FW,\leftarrow} \neq 0$ and $s_{SW,\rightarrow} = 0$ or $s_{FW,\rightarrow} = 0$ and $s_{SW,\rightarrow} \neq 0$.

The adopted set of boundary conditions is useful for demonstrating the interplay between the different modes supported by the plasma. For later, more practical applications more convenient boundary conditions (e.g., matching 2 of the relevant electric field components, which is easier to implement) are likely to be preferred. By imposing a jump condition on the derivative of the field components while ensuring continuity of the 2 retained electric field components, a simple sheet current antenna can be included. In that case, purely outgoing wave conditions are commonly imposed at the interface with the main plasma.

The expression for the Ponderomotive acceleration reveals that the various waves supported by the plasma impact differently on the density. Figures 3 and 4 show the roots of the dispersion equation and the corresponding exponent of the density expression for the earlier considered

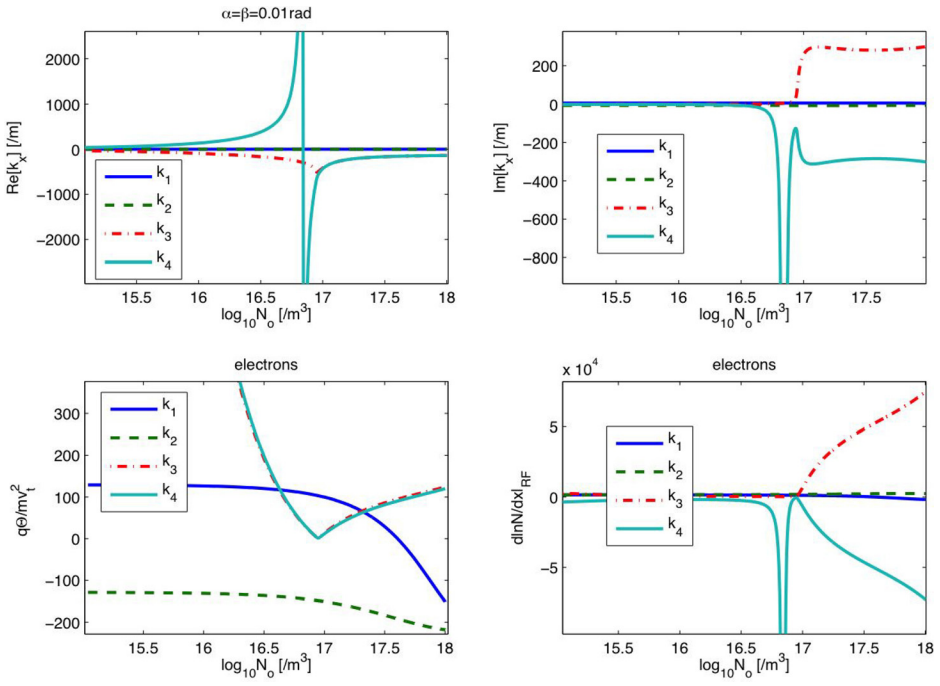

FIG. 3. Dispersion roots, Ponderomotive potential, and density decay rate as a function of the log_{10} of the density for $\alpha = \beta = 0.01$ rad.

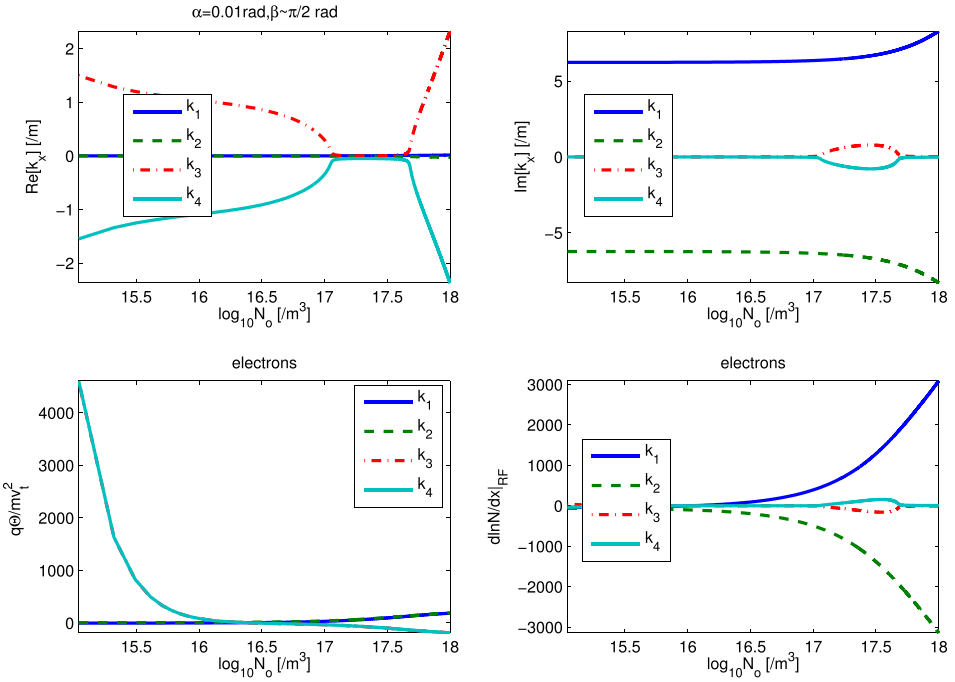

FIG. 4. Dispersion roots, Ponderomotive potential, and density decay rate as a function of the log_{10} of the density for $\alpha = 0.01$ rad and $\beta = 1.57$ rad.

parameters and for the 2 limiting cases $\alpha = \beta = 0.01$ *rad* (representative for the magnetic field nearly parallel to the wall) and $\alpha = 0.01$ rad and $\beta = 1.57$ rad (field nearly perpendicular to the wall) when scanning the density. The slow wave has a much more pronounced impact than the fast wave has due to the difference in the magnitude of their respective wave numbers. On the scale of the slow wave, the fast wave is hardly noticed on the top plots showing the 4 dispersion equation roots. The fact that the dispersion equation has odd order terms making that the roots do not appear as pairs $(k_x, -k_x)$ is clearly seen. The lower hybrid resonance is recognized as the region where the slow wave becomes propagative in Fig. 3 for densities a bit lower than $10^{17}/m^3$. It was already discussed in the previous work that the presence of the lower hybrid resonance has repercussions both on the physics of the wave dynamics close to the launcher and on the numerical challenge arising when incorporating it in the model.

The shown curves are somewhat misleading: The amplitude of the wave field is imposed here, while in practice waves can only have an impact if they *are* actually excited. Furthermore, the global effect on the density is the result of the sum of all waves and not that of a single mode. In practice, the density depletion is more modest than suggested by the curves for the individual wave modes because of the fact that generally several modes coexist to ensure the boundary condition is satisfied by the total $\vec{E}$-field; as there is no damping in the system, an incoming wave hitting the metallic wall is undergoing total reflection so a pure incoming eigenvector will unavoidable excite at least one of the outgoing modes. The pronounced difference between the impact of the slow and the fast wave is vastly diminished when the slow wave only carries modest energy, the typical wave intended to be excited in the RF domain being the fast wave. When discussing the solution of the full problem later in the text, this effect will be accounted for. The here presented curves mainly give an idea of the potential of waves to modify the density.

C. Continuity equation

Making an identical splitting of fast and slow time scales as was done for the equation of motion, the relevant continuity equations are obtained. The slow time scale continuity equation reads

$$\frac{\partial N_o}{\partial t} + \nabla.(N_o \vec{v}_o) + \frac{1}{2} Re\left[\nabla.\left(N_1^* \vec{v}_1\right)\right] = 0, \qquad (17)$$

in which the perturbed velocity and density appear in the last term; this quasilinear term is the net contribution of the fast time scale wave dynamics to the slow time scale equation. The perturbed velocity was already specified earlier. Conform with the earlier made assumptions, the slow time scale continuity equation will be solved in the limit $\partial/\partial t \to 0$ so one gets

$$N_o \frac{\partial v_{//}}{\partial x_{//}} + v_{//} \frac{\partial N_o}{\partial x_{//}} + \vec{v}_{\perp,o}.\nabla_\perp N_o + \frac{1}{2} Re\left[\frac{d}{dx}\left(N_1^* v_{1,x}\right)\right] = 0, \qquad (18)$$

in which $\nabla.\vec{v}_{\perp,o} = 0$ was used and where the last term in the above only contains the x-derivative term since the perturbed quantities vary as $exp[i(k_y y + k_z z - \omega t)]$ in the directions perpendicular to the wall and hence quadratic quantities of the form $Re[A^* B]/2$ are independent of y and z when a single set (k_y, k_z) of modes is looked at. Note that in the absence of RF waves and if the confining magnetic field is strong so that the perpendicular drift velocity is modest, $N_o v_{//}$ is roughly a constant. In that limiting case, the parallel current across the region of interest is constant. More generally it is not: due to the gradients, current can partly flow sideways and does not need to flow straight into the wall and launcher.

Using the equation of motion to eliminate the parallel velocity gradient, the above can be reformulated. The result is

$$\left[v_{//}^2 - v_t^2\right]\frac{\partial lnN_o}{\partial x_{//}} + v_{//}\vec{v}_\perp.\nabla_\perp lnN_o - \frac{q}{m}\frac{\partial \Phi}{\partial x_{//}} - \frac{\partial \Theta}{\partial x_{//}} + \frac{v_{//}}{2N_o}Re\left[\frac{d}{dx}N_1^* v_{1,x}\right] = 0. \quad (19)$$

The coefficient in front of the leading term states that the density grows or decays depending on whether the flow is faster or slower than the thermal flow. In the absence of a rapidly varying field and for a strong static magnetic field, this equation reduces to the one already adopted in Ref. 1 where the wave equation was solved without accounting for the wave induced corrections on N_o. Whereas the parallel flow equation suggests that the ion density can grow very large when the electron density is dropping, the combined equation learns that ion flow velocities satisfying the Bohm criterium tend to decay towards metallic walls. As the electron flow velocity is typically much smaller than the electron thermal velocity close to the wall, the Boltzmann expression is recaptured in that particular limit.

An expression for the perturbed velocity was evaluated in Appendix A. The perturbed density obeys the fast time scale continuity equation

$$-i\omega N_1 + \nabla.[N_o\vec{v}_1 + N_1\vec{v}_0] = 0. \quad (20)$$

It may be argued—rightfully—that the slow time scale continuity equation should in general allow for source/loss terms so that the density variation is not just due to convection. Especially, the plasma edge processes, such as ionisation, recombination, or recycling, are likely to have an impact on the density profile. When focusing on the dynamics in a limited volume (such as the sheath formed close to a metal), these effects can implicitly be accounted for by a properly *prescribed* plasma composition. When modeling the wave-particle interaction macroscopically (e.g., looking at the density in the whole region close to the launcher) such effects play a key role.

A common example for tokamak applications is the cross-field diffusion that *leaks* particles across the last closed flux surface so that the source that injects particles into a magnetic field line is of the form $\partial/\partial x_\perp[D_\perp\partial/\partial x_\perp[N_o]]$, where $x_\perp$ is the magnetic surface labeling parameter, to be identified with one of the 2 variables $x_{\perp,1}$ or $x_{\perp,2}$ introduced before (see, e.g., Ref. 29). A qualitative estimate of the solution of the simplest possible steady state continuity equation with source

$$\frac{\partial}{\partial x_{//}}\left[v_{//}N_o\right] = \frac{\partial}{\partial x_\perp}D_\perp\frac{\partial}{\partial x_\perp}N_o$$

then shows that the density is essentially proportional to $exp[\alpha_\perp x_\perp]$ where $\alpha_\perp = (v_{//}/[D_\perp L_{//}])^{1/2}$ in the perpendicular direction, while in the parallel direction it varies crudely as $exp[\alpha_{//}x_{//}]$ with $\alpha_{//} = D_\perp/[L_\perp^2 v_{//}]$. The exponential decay length across the magnetic field lines behind the last close flux surface is typically of order of a few centimeters: for a deuterium plasma, assuming an edge temperature of $T = 10\,\text{eV}$, taking the parallel scale length $L_{//}$ to be 10 m and $D_\perp = 1\ \text{m}^2/\text{s}$, one gets $1/\alpha_\perp \approx 0.02\,\text{m}$.

The density gain or loss through ionization or recombination is described via the reaction rate of the process modeled and involves the densities of the species taking part in the interaction, i.e., $\partial N_i/\partial t|_{k,ij} = \pm R_{k,ij}N_iN_j$ where the "+" is relevant for the "receiving" specie and the "-" for the "donating" specie. Incorporating a large set of relevant processes and their respective reaction rates, Wauters successfully developed a model for the birth of plasma under the influence of RF waves, which enabled him to get a grip on the dynamics of ion cyclotron wall conditioning and RF assisted plasma startup.[30,31]

The so far described sources scale with the density. Aside from this kind of sources, the density may change due to the processes that are independent of the local density. When aiming at making realistic macroscopic predictions on wave induced density depletion, all such effects should be included in the model. When formulating the problem in 2D, such description is both natural and essential. At the current stage, such effects are merely mocked up by a simple source term in the continuity equation.

D. Slow time scale wave equation: Poisson's equation

Since the slow time scale magnetic field is constant in time, the electric field can be derived from a potential. The law of Gauss then reduces to the Poisson equation

$$\Delta\Phi = \frac{e}{\epsilon_o}\left[N_{e,o} - \sum_i Z_i N_{i,o}\right]. \quad (21)$$

E. Scheme

A sketch of the scheme adopted for solving the set of linear and nonlinear equations is given in Fig. 5. For given ion and electron density profiles, the electrostatic potential as well as the RF electric field can be found. The latter allows to evaluate the Ponderomotive force, which—together with all other relevant forces—is fed into the slow time equation of motion yielding $\vec{v}_o$. The perturbed velocity $\vec{v}_1$ is known in terms of the RF electric field. Locally, the perpendicular part of Klima's equation of motion is solved analytically and the rapid cyclotron oscillation is removed so that only the perpendicular drift motion is retained. The parallel velocity is found solving the parallel component of the equation of motion numerically. Using the found slow and fast time scale velocities, the continuity equations allow to update the densities. By iteratively going through this loop, the stationary state density consistent with the electric field pattern and electrostatic potential is obtained.

III. ADOPTED EQUATIONS AND NUMERICAL PROCEDURE

Due to the presence of the strong, static and constant magnetic field and the fact that the magnetic field cannot accelerate particles along its field lines, the slow time scale equation of motion can be solved explicitly for the perpendicular aspects of the motion forced by $\vec{B}_o$ while the parallel motion is a differential equation with $x_{//}$ as the independent variable. On the other hand, the presence of a metallic wall yields dynamics essentially in the x-direction perpendicular to the wall. It will be assumed in this paper that $\partial/\partial y \approx \lambda_y$

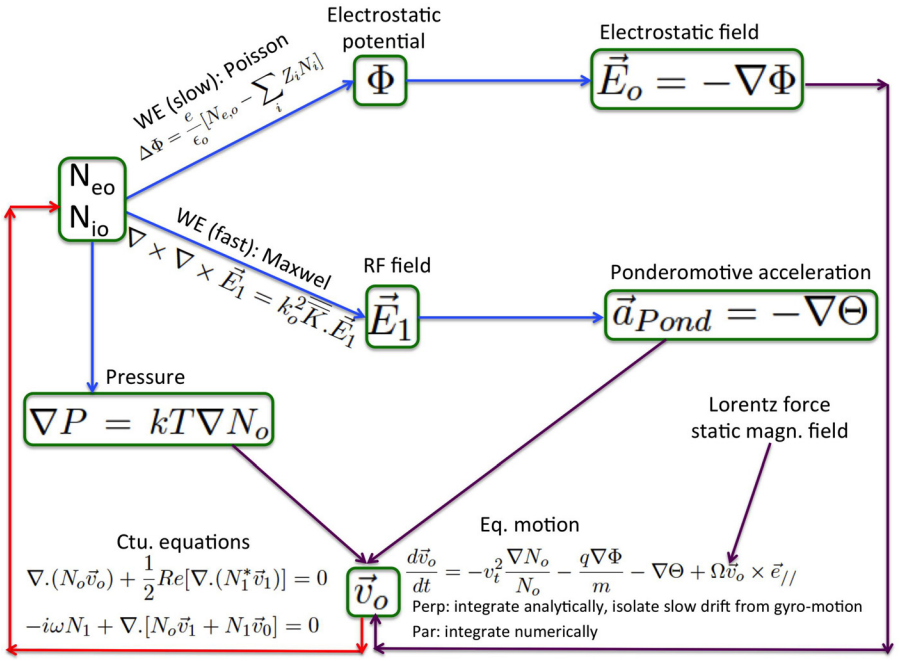

FIG. 5. Sketch of the adopted scheme iterating over the fast and slow time scale equations.

and $\partial/\partial z \approx \lambda_z$ and that the typical scale lengths over which the zero order quantities vary are long compared to, e.g., the characteristic scale lengths of the excited RF waves. Strictly, the earlier described equations allow application of the proposed method to 2D or 3D application and thus allow to have the full (k_y, k_z) spectrum for the fast time scale and proper derivatives for the slow time scale variables, removing the need to *impose* prescribed variations along the metallic wall and allowing to find them self-consistently.

The differential operators needed in the various slow time scale equations now reduce to

$$\begin{pmatrix} \frac{\partial}{\partial x_{\perp,1}} \\ \frac{\partial}{\partial x_{\perp,2}} \\ \frac{\partial}{\partial x_{//}} \end{pmatrix} = \begin{pmatrix} \mathcal{R}_{11} \\ \mathcal{R}_{21} \\ \mathcal{R}_{31} \end{pmatrix} \frac{d}{dx} + \begin{pmatrix} \mathcal{R}_{12} \\ \mathcal{R}_{22} \\ \mathcal{R}_{32} \end{pmatrix} \lambda_y + \begin{pmatrix} \mathcal{R}_{13} \\ \mathcal{R}_{22} \\ \mathcal{R}_{33} \end{pmatrix} \lambda_z, \quad (22)$$

and hence the relevant equations are:

- The slow time scale continuity yielding $v_{//}$

$$A_{v_{//}}(x)\frac{dv_{//}}{dx} + B_{v_{//}}(x)v_{//} + C_{v_{//}}(x) = 0, \quad (23)$$

where

$$A_{v_{//}}(x) = \mathcal{R}_{31}N_o$$

$$B_{v_{//}}(x) = \mathcal{R}_{31}\frac{dN_o}{dx} + \frac{3}{2}\left(\mathcal{R}_{32}\lambda_y + \mathcal{R}_{33}\lambda_z\right)N_o$$

$$C_{v_{//}}(x) = \left[v_{drift,\perp 1}\mathcal{R}_{11} + v_{drift,\perp 2}\mathcal{R}_{21}\right]\frac{dN_o}{dx} + \left[v_{drift,\perp 1}\left(\mathcal{R}_{12}\lambda_y + \mathcal{R}_{13}\lambda_z\right) + v_{drift,\perp 2} \times \left(\mathcal{R}_{22}\lambda_y + \mathcal{R}_{23}\lambda_z\right)\right]N_o + \frac{1}{2}Re\left[\frac{d}{dx}\left(N_1^* v_{1,x}\right)\right].$$

A "density source" term $-D_\perp/\lambda_{SOL}^2 N_o$, where $D_\perp$ is the diffusion across magnetic field lines and $\lambda_\perp$ is a typical decay length of the density in the scrape-off layer, can be added to $C_{v_{//}}$ when modeling macroscopic decay. As a boundary condition, it seems natural to assume that the parallel flow is known at the entrance of the region of interest. In the spirit of dynamics close to metallic objects, $v_{//}$ is taken to be of the order of the thermal velocity for the ions while the electron flow is chosen to guarantee that no steady state current enters the region of interest, i.e., $v_{//,e}N_e = -\sum_i Z_i N_i v_{//,i}$.

- The slow time scale parallel equation of motion yielding the (logarithm of the) density N_o

$$A_{lnN_o}(x)\frac{dlnN_o}{dx} + B_{lnN_o}(x)lnN_o + C_{lnN_o}(x) = 0, \quad (24)$$

where

$$A_{lnN_o}(x) = v_t^2\mathcal{R}_{31}$$

$$B_{lnN_o}(x) = v_t^2\left(\mathcal{R}_{32}\lambda_y + \mathcal{R}_{33}\lambda_z\right)$$

$$C_{lnN_o}(x) = \mathcal{R}_{31}\frac{d}{dx}\left[\frac{q}{m}\Phi + \Theta\right] + \left[\mathcal{R}_{32}\lambda_y + \mathcal{R}_{33}\lambda_z\right]\left[\frac{q}{m}\Phi + \Theta\right] + \left(v_{drift,\perp 1}\mathcal{R}_{11} + v_{drift,\perp 2}\mathcal{R}_{21} + v_{//}\mathcal{R}_{31}\right)\frac{\partial v_{//}}{\partial x} + \frac{1}{2}\left(\mathcal{R}_{32}\lambda_y + \mathcal{R}_{33}\lambda_z\right)v_{//}^2 + \frac{1}{2}\left[v_{drift,\perp 1} \times \left(\mathcal{R}_{12}\lambda_y + \mathcal{R}_{13}\lambda_z\right) + v_{drift,\perp 2}\left(\mathcal{R}_{22}\lambda_y + \mathcal{R}_{23}\lambda_z\right)\right]v_{//},$$

in which λ_y and λ_z are assumed to be the common local derivatives of N_o, $v_{//}^2$, Φ and Θ in the y and z direction, respectively. Integrating the logarithm of the density rather than the density itself proved to be numerically more stable. It is assumed that charge neutrality is guaranteed at the interface with the main plasma. As the boundary condition, the electron and ion densities are imposed

at that location. Consistent with the alternative Eq. (19), the above can be substituted for

$$A_{lnN_o}(x) = \left[v_{//}^2 - v_t^2\right]\mathcal{R}_{31} + v_{//}[v_{drift,\perp 1}\mathcal{R}_{11} + v_{drift,\perp 2}\mathcal{R}_{21}]$$
$$B_{lnN_o}(x) = [v_{//}^2 - v_t^2][\mathcal{R}_{32}\lambda_y + \mathcal{R}_{33}\lambda_z] + v_{//}[v_{drift,\perp 1}[\mathcal{R}_{12}\lambda_y + \mathcal{R}_{13}\lambda_z] + v_{drift,\perp 2}[\mathcal{R}_{22}\lambda_y + \mathcal{R}_{23}\lambda_z]]$$
$$C_{lnN_o}(x) = -v_{drift,\perp 1}\left[\mathcal{R}_{11}\frac{\partial v_{//}}{\partial x} + \frac{v_{//}}{2}\left[\mathcal{R}_{12}\lambda_y + \mathcal{R}_{13}\lambda_z\right]\right] - v_{drift,\perp 2}\left[\mathcal{R}_{21}\frac{\partial v_{//}}{\partial x} + \frac{v_{//}}{2}\left[\mathcal{R}_{22}\lambda_y + \mathcal{R}_{23}\lambda_z\right]\right] - \frac{q}{m}\left[\mathcal{R}_{31}\frac{\partial \Phi}{\partial x} + [\mathcal{R}_{32}\lambda_y + \mathcal{R}_{33}\lambda_z]\Phi\right] - \mathcal{R}_{31}\frac{\partial \Theta}{\partial x} + \frac{v_{//}}{2N_o}Re\left[\frac{d}{dx}\left(N_1^* v_{1,x}\right)\right].$$

Note that the last term in the above points to a weakness in the model: when $N_o \to 0$, $C_{lnN_o} \to \infty$. Rather than being physically meaningful, this divergence is a testimony of the fact that the linearization—which assumes $N_1 \ll N_o$—breaks down and needs to be replaced by a suitable alternative.

- The slow time scale wave equation yielding the potential Φ:

$$\frac{d^2\Phi}{dx^2} + \left(\lambda_y^2 + \lambda_z^2\right)\Phi = \frac{e}{\epsilon_o}\left[N_e - \sum_i Z_i N_i\right]. \quad (25)$$

For a given N_o, imposing $\Phi = 0$ at x_p (the integration domain of interest ends where charge neutrality is recaptured) and a finite value $\Phi = \Phi_{wall}$ at x_{wall} yields a unique solution. This set of boundary conditions is useful in case some external mechanism (e.g., grounding) is imposing the voltage on the vessel wall. More generally, the wall voltage is a free parameter, however. Other choices were considered as well. To ensure the potential reaches a constant value at the interface with the plasma, imposing a vanishing derivative of Φ was, for example, also a handy boundary condition to ensure charge neutrality is gradually removed towards the interface with the rest of the plasma.

- The fast time scale wave equation yields the perturbed electric field $\vec{E}$; details can be found in Sec. II B. Once $\vec{E}$ is known, the components of the perturbed velocity can be computed, and Θ can be found. The perturbed density follows from the fast time scale continuity equation:

$$A_{N_1}(x)\frac{dN_1}{dx} + B_{N_1}(x)N_1 + C_{N_1}(x) = 0 \quad (26)$$

with

$$A_{N_1}(x) = v_{drift,\perp 1}\mathcal{R}_{11} + v_{drift,\perp 2}\mathcal{R}_{21} + v_{//}\mathcal{R}_{31}$$
$$B_{N_1}(x) = \mathcal{R}_{31}\frac{dv_{//}}{dx} + i\left[-\omega + v_{\perp,1}[k_y\mathcal{R}_{12} + k_z\mathcal{R}_{13}] + v_{\perp,2}[k_y\mathcal{R}_{22} + k_z\mathcal{R}_{23}] + \frac{v_{//}}{2}\left[k_y\mathcal{R}_{32} + k_z\mathcal{R}_{33}\right]\right]$$
$$C_{N_1}(x) = N_o\left[\frac{dv_{1,x}}{dx} + ik_y v_{1,y} + ik_z v_{1,z}\right] + v_{1,x}\frac{dN_o}{dx} + \left(v_{1,y}\lambda_y + v_{1,z}\lambda_z\right)N_o.$$

A suitable option for the boundary condition of this first order equation is to assume that the density N_1 is known at some reference position. Since the wave field modifies the density and one expects the deviation to be larger for larger fields (see Eq. (12)), one can—however—not simply force N_1 to have a prescribed density. As will be explained next, setting up an iterative scheme not only allows to solve this issue but equally provides an elegant solution for tackling the set of equations at hand. Alternatingly imposing N_1 to be imposed at the wall or at the plasma interface and taking it to be the value found in the previous iteration allows to avoid having to impose a specific value for N_1 at any place.

Most of the equations are linear equations for individual quantities but are nonlinear equations in terms of the various unknown quantities. Rather than solving all (linear and nonlinear) equations simultaneously, the set of equations can be solved *iteratively* addressing the dependence of the variables one by one and hence solving a series of linear equations at each iteration; a similar philosophy was adopted by Louche and by Meneghini.[5,24]

Aside from the fast and slow time scale wave equations, all relevant equations are first order differential equations of the form

$$A\frac{dF}{dx} + BF + C = 0. \quad (27)$$

The solution of this first order differential equation is

$$F(x) = \left[F(x_{ref}) - \int_{x_{ref}}^{x} dx\frac{C}{A}\exp\left[\int_{x_{ref}}^{x}\frac{B}{A}dx\right]\right]\exp\left[-\int_{x_{ref}}^{x}\frac{B}{A}dx\right]. \quad (28)$$

IV. A FEW PRELIMINARY EXAMPLES

In spite of the fact that the dynamics of convective cells is inherently multidimensional and thus strictly falls outside the possibilities of a 1D model, providing a few examples to illustrate how the waves and the plasma interact close to launchers allows to point out a number of the characteristic ingredients of the wave-particle interaction. The following parameters were considered: 5% hydrogen in a deuterium majority plasma, electron and ion temperature $T_e = T_i = 15$ eV, magnetic field strength $B_o = 2.5$ T at the antenna and a driver frequency of $f = 51$ MHz (as mentioned earlier, these values are relevant for JET's A2 RF antenna region). Waves excited at the launchers, carrying power through the low density edge region and subsequently hitting the metallic wall of the vessel are considered but the magnetic field is not required to be parallel to the wall. For the presented examples, the magnetic field direction is determined by $\alpha = \beta = 0.5$ rad. On the fast time scale the waves enter the region of interest obliquely to the wall; we chose $k_y = 5$/m and $k_z = 6$/m. Various electron densities (ranging from 5×10^{16}/m^3 to 5×10^{17}/m^3) were considered at the interface with the region where charge neutrality is regained. Loosely inspired on the Bohm criterium relevant very close

to metallic walls, the ion velocities at the interface of the region of interest with the main plasma are prescribed to be the thermal velocity multiplied by a factor of order 1; the electron parallel flow velocity was chosen to ensure that there is no slow time scale current density at the entrance of the integration region ($J \approx -eN_e v_{//} + \sum_i Z_i N_i v_{//,i} = 0$). The electrostatic potential is 0 at that location. Depending on whether charge neutrality is assumed or not, the potential at the wall is given a zero or nonzero value.

As a first example, Fig. 6 depicts the density of the electrons and ions for various values of the perturbed electric field amplitude $|\vec{E}|$. Poisson's equation was *not* solved, i.e., charge neutrality was assumed so the density modification is solely due to the presence of a finite fast time scale electric field. The slow time scale gradients parallel to the wall were assumed to be negligibly small. The antenna is located almost at the mouth of the antenna region interconnecting to the "outer plasma." It is modeled as a simple current sheet with $J_y = J_z = ct$ where the constant is determined by adjusting it to a desired electric field amplitude at the interface with the main plasma. The metallic back wall of the box is 19 cm away from the antenna to the left, and the main plasma is 1 cm to the right of it. At the latter, the density is prescribed. A value of $N_e = 5 \times 10^{17}/\mathrm{m}^3$ was taken. To include the effect of the wall in the computation and opposite to what is usually done, the $\vec{E}$ fields are not computed towards the main plasma but rather towards the back wall to simultaneously study the effect of a launcher and a reflecting wall. Whereas the ions are hardly affected by $|\vec{E}|$ (only the result for $|\vec{E}| = 0$ is shown since the other ion curves almost overlap), the electron density is clearly depleted when $|\vec{E}|$ is increased. Consistent with the fact that the Ponderomotive potential involves the square of the electric field magnitude, the strongest decrease is close to the antenna and the density modification is strongest close to the antenna. For the parameters considered, the electric field—not shown—decreases somewhat stronger than linearly away from the antenna and becomes small close to the wall since the magnetic field lines obliquely fall on it, forcing all components perpendicular to $\vec{B}_o$ to become small in spite of the fact that both a fast and slow wave are excited by the antenna. Recall that a magnetised plasma is gyroscopic and that the $\vec{E}$ components perpendicular to $\vec{B}_o$ are closely coupled; the strength of the coupling of the parallel and perpendicular components depends on the angle at which the wave propagates but is typically weaker.

Next, the density modifications for 4 different values of the angle α are depicted. A common electric field strength of 150 kV/m was considered loosely based on the fact that voltages of a few tens of kV are routinely imposed on RF antennas and that the—usually grounded—side and back walls of the antenna box are often only several cm ($\approx$0.1 m) away from the straps. A density of $N_o = 5 \times 10^{16}/\mathrm{m}^3$ was assumed at the interface. Figure 7 shows that the density depletion is gradually more pronounced when α increases. For the highest values of α, the magnetic field is nearly parallel to the metallic wall (the limiting case $\alpha = \pi/2$ cannot be modeled since then there is no projection of $x_{//}$ onto x and hence the adopted equation for the parallel flow cannot be used to predict parallel flow modifications perpendicular to the wall; in that particular case knowing the density at the edge does not allow predicting its value elsewhere). The density depletion observed in the figure for $\vec{B}_o$ nearly parallel to the wall is at least partly the consequence of the geometrical fact that the distance traveled along the magnetic field line is much larger than that of the distance traveled perpendicular to the wall for a given width perpendicular to the wall of the examined region.

Quite generally, waves hit the wall obliquely and hence k_y and k_z are nonzero. This has repercussions for the wave-particle interaction. Figure 8 shows the density consistent with k_y ranging from -40/m to $+40$/m. As before, the ion response to the changing conditions is much weaker than the electron response. Only the majority density is plotted and only for 1 value of k_y. The electron density deviation from the value of $2 \times 10^{17}/\mathrm{m}^3$ imposed at the interface with the main plasma differs for every k_y, depending on what the RF wave pattern looks like exactly. Although the density most

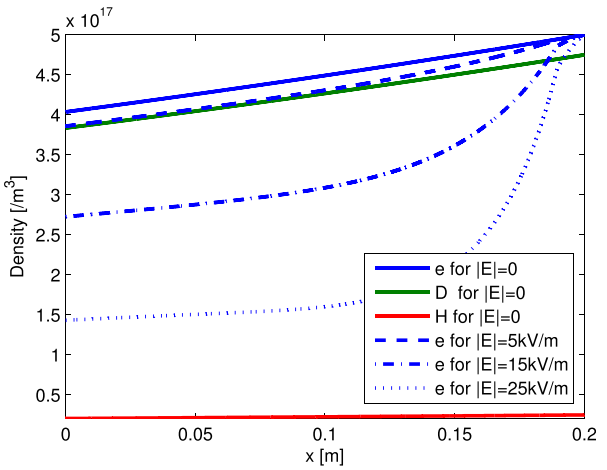

FIG. 6. Dependence of the density profile close to the antenna for various RF electric field strengths. The full lines are the densities in absence of the RF field. While the ion response is almost unvaried, the electron response depends critically on the amplitude of the RF electric field. The profiles for $|E| = 5$, 15, and 25 kV/m are depicted.

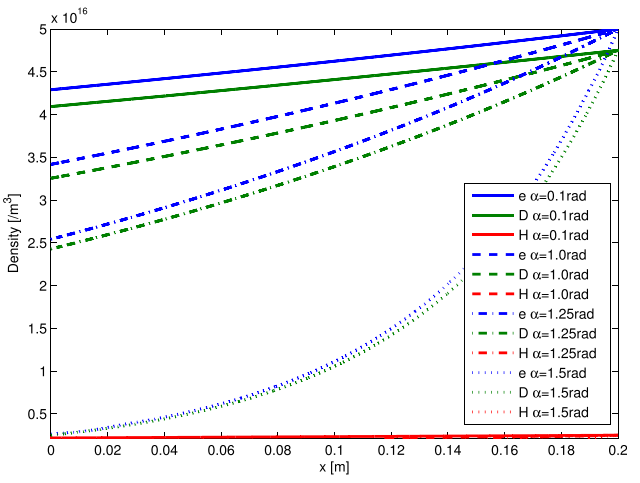

FIG. 7. Macroscopic RF induced density depletion for various values of the angle α.

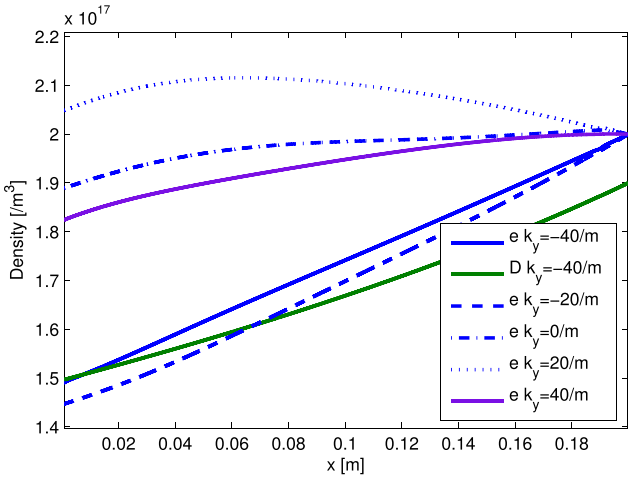

FIG. 8. Macroscopic RF induced density depletion for various k_y.

commonly decays when leaving the antenna region, the figure shows it occasionally *increases* instead.

Figure 9 shows the density modification close to the wall. Since the field tangential to the wall vanishes, 2 of the 3 field components need to vanish there. Due to the presence of the magnetized plasma, all field components are coupled. As a result, the whole field tends to be much smaller close to walls and typical values for $|E|$ at microscopic distance from the wall are much smaller than what was considered for the macroscopic examples. Furthermore, opposite to the previous examples, charge neutrality is not assumed and a finite voltage difference between the main plasma—where charge neutrality does hold—and the wall is allowed. The corresponding electrostatic field is found solving the Poisson equation using the zero order densities as input. The model presented here does not permit to predict the wall potential and hence a value needs to be imposed. Evidently, the profile of the potential found depends on the input taken. Assuming a very small but finite value for the derivative of the potential at the interface with the main plasma, the value for the wall

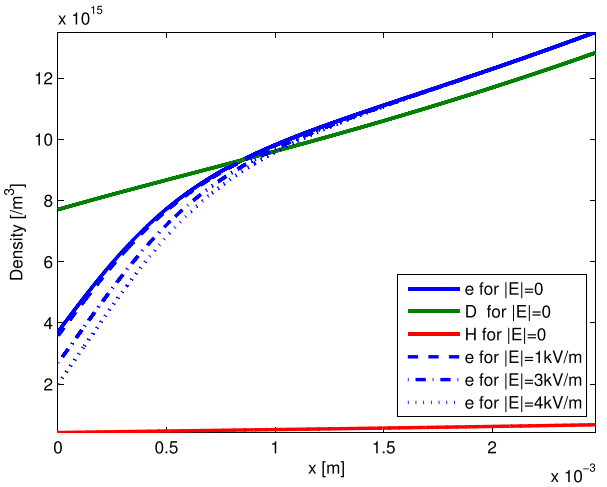

FIG. 9. Dependence of the density profile close to the wall for various RF electric field strengths. The full lines are the densities in absence of the RF field. While the ion response is almost unvaried, the electron response depends critically on the amplitude of the RF electric field. The profiles for $|E| = 1$, 3, and 4 kV/m are depicted.

potential is left unspecified. Since the Ponderomotive potential varies nonlinearly with $|E|$, the density responds nonlinearly and the voltage drop across the region is equally nonlinear. At negligibly small RF field, the drop is about 12 V. This value is crudely unchanged when increasing the field up to $|E| = 3\text{kV/m}$ but when $|E| = 4\text{kV/m}$ it almost doubled to 20 V. Beyond that value, the density at the wall drops quickly and linearization breaks down: although the relative magnitude of the perturbed and the zero order density is acceptably low (a few percent) at the interface when $|E|$ reaches 4 kV/m, it becomes of similar amplitude at the wall side. When the RF field becomes larger, the linearization breaks down already further away from the wall. It is, however, reasonable to assume the predicted trend subsists: RF waves tend to depopulate the region close to the metal wall. For the specific case of waves in the lower hybrid range of frequencies, Chan and Meneghini demonstrated that sufficiently large amplitude waves can push the density to zero.[4–6] Figure 10 illustrates how the density, the perturbed density, the parallel velocity and the potentials (relevant for the electrons) vary as a function of the distance to the wall for $|E| = 4\text{kV/m}$. In view of the violation of the linearization, it seems useful to explore the potential of a model that *does* account for the fact that there are 2 different time scales in the problem, but that does *not* rely on the assumption that the perturbation is small.

Figure 11 illustrates the iteration scheme adopted to describe the wave-particle interaction for a few key quantities; the flow diagram given in Fig. 5 is followed. First, the electrostatic potential and corresponding density are found by neglecting the RF electric field. The nonlinear equations are solved by gradually switching on the magnitude of the nonlinear amplitude terms. Once at full value, the RF terms are also gradually switched on. Finally, when all terms have reached their full amplitude, a number of iterations are added up to the point where none of the quantities still vary from one iteration to the next. As the reached state satisfies the non-linear equations, the found solution is considered to be the stationary state solution to the posed non-linear wave-particle interaction problem.

V. CONCLUSIONS AND DISCUSSION

In the present paper, a model is presented to study the interaction of RF waves and a plasma. The focus is on the region close to the launcher. In view of the vastly different time scales involved, a 2-time scale model has been set up. On both time scales, it consists of a wave equation, an equation of motion, and the continuity equation. The slow time scale dynamics is influenced by the fast time scale physics through quasilinear modifications. The fast time scale equation of motion is solved analytically as a driven problem, and the corresponding wave fields and fast time scale density modification are computed starting from the same assumption. The perpendicular dynamics of the slow time scale equation of motion is equally solved analytically, implicitly assuming the static magnetic field is strong and that its gradients can be neglected as a first approximation. The parallel equation of motion needs to be solved numerically, except

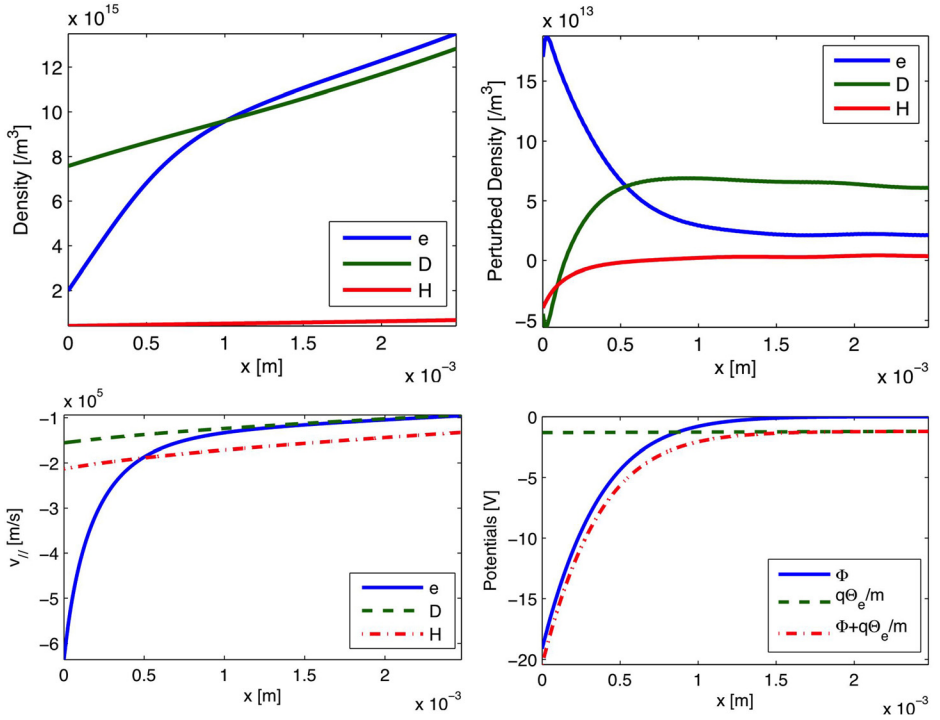

FIG. 10. Macroscopic density, perturbed density, parallel velocity, and potentials relevant for the electrons for $|E| = 4\,\mathrm{kV/m}$.

for the case when drifts can be neglected. Discarding perpendicular drifts altogether and just focusing on the parallel dynamics allows to integrate the equation of motion by hand and yields a generalization of the Boltzmann density expression commonly adopted for the electrons. In that expression, the parallel energy, the electrostatic potential, and the Ponderomotive potential play a similar role. Just like the dependence of the electrostatic potential on the sign of the charge makes that ions and electrons respond differently, the difference in mass of the species has a direct implication on the magnitude of the Ponderomotive potential for the various types of species. Moreover, the required wave polarization has repercussions on which species are affected: For frequencies in the ion cyclotron frequency range, the electron dynamics is dominantly controlled by the parallel electric field while the ions are mainly affected by the perpendicular components. To the exception of the case where an ion cyclotron resonance is crossed in the region of interest (for which case strictly a kinetic model—see, e.g., Refs. 32 and 33 —is required as the cold plasma expressions artificially predict an infinite response), the Ponderomotive effect is not as important for ions as it is for electrons. The adopted fast time scale wave equation is the standard one; it relies on the cold plasma dielectric tensor but takes the actual densities into

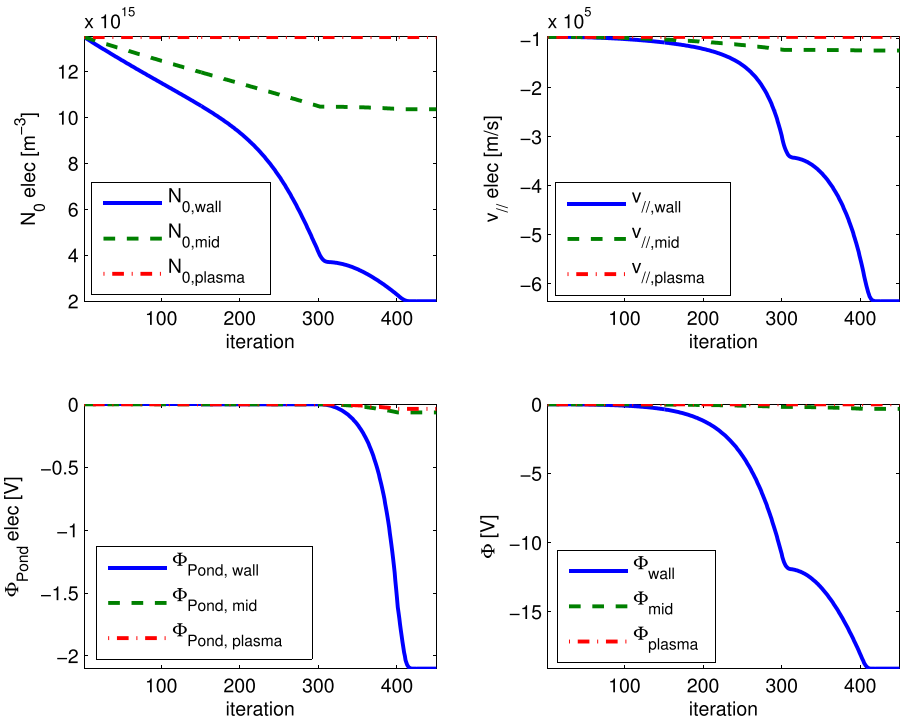

FIG. 11. Values of various quantities as a function of the iteration step.

account for the electrons as well as the ions. For the slow time scale wave equation, it is assumed that a steady state has been reached so that the corresponding electric field is the gradient of a potential as a consequence of Faraday's law. Hence, the full electromagnetic equation does not need to be solved on that time scale but can be replaced by Poisson's equation. The electrostatic potential is nonzero if charge neutrality is violated.

A key finding of this paper is that the earlier found expression for the Ponderomotive potential in the presence of a strong magnetic field plays a role similar to the electrostatic potential for wave induced density modification. This result was already found by Chan for lower hybrid waves.[4] In Ref. 1, the accent was on computing the perpendicular drifts brought about by the Ponderomotive force. This allowed to demonstrate that variations of the electric field amplitude perpendicular to the antenna straps cause poloidal drifts along the launcher and that the strong gradients at the antenna strap tips cause radial flows towards and away from the antenna. In that paper (which described effects that are beyond a 1D description), the back-reaction of the electric field through the Ponderomotive potential was not incorporated in the density modification. This back-reaction was the main subject of the present paper, be it that the model was kept 1-dimensional here so that variations of fast as well as slow time scale variables along the wall or launcher are prescribed rather than computed self-consistently. Ions and electrons are treated on the same footing but respond differently to the presence of the potentials. At the plasma side, it is imposed that no net current flows into the region of interest.

The resulting set of equations is a mix of linear and nonlinear equations. Rather than solving the actual nonlinear problem, an iterative scheme was set up to solve the nonlinear problem as a series of linear ones. The various gradients in the equations of motion and the continuity equation are gradually switched on so that the parallel velocity, density, potential, and field can be approximated at each step by the value found in the previous iteration. Adding supplementary iterations after the various derivatives are at full strength allows reaching a steady state solution. In view of the nonlinearities, the equations solved remain numerically touchy in some cases, however. As a result, many iterations (of the order of 1000) are needed before reaching a steady state. Also, a high number of grid points is often required. For the present examples, up to 60 000 grid points are taken for the first order equations; the wave equations typically require only a few hundred grid points. This substantial number of points is needed to capture the behaviour when the density approaches zero. Although it does not pose a particular problem for the present 1D treatment which requires modest CPU time whatsoever, it both points to the fact there is a need for improvement of the numerical scheme when the wave-plasma interaction is to be modeled in more than a single dimension, and underlines the fact that the linearisation locally breaks down and the physics model needs to be upgraded to properly describe regions where that happens. The difficulty of solving the nonlinear set of equations relevant for high amplitude waves in low density regions close to metallic walls has already been noticed when adopting simpler models: Van Compernolle *et al.*[34] experimented with implementing the sheath boundary condition due to Myra and D'Ippolito[35–43] and was confronted with non-convergence when the RF power density was too high.

Further upgrading the model is a must. The here presented set of equations has been applied in 1D while convective cells created in front of launchers are multidimensional. Retaining rather than neglecting the omitted derivatives and adding proper "source" terms would allow to assess the dynamics in 2D or 3D and can be done in a macroscopic region. This would offer a method for describing the wave induced density depletion in the antenna box, as was demonstrated by a first, rather crude example. Such an approach was already tested in Ref. 1 without iterating on the obtained density and fast time scale wave field. Since zero order flows are formed, the cold plasma dielectric tensor (which assumes $\vec{v}_o = 0$) can strictly no longer be used so, ultimately, also the fast time scale wave equation needs to be upgraded to the set of equations mentioned in that paper. More work to upgrade the physics model and to include 2D and 3D effects is reserved for future work.

As a finishing note, one needs to remind that the here presented model has the strengths but also the weaknesses that come along with the adopted fluid model.[7] Kinetic modeling remains necessary to obtain more detailed insight in certain aspects that involve deviations away from Maxwellian distributions. The main advantage of fluid modeling compared to kinetic modeling is that it requires less computer time and computer memory. Another obvious limitation is that the derivation of the Ponderomotive force rests on the assumption that the Taylor series expansion of the field can be truncated after the linear term. In the antenna box, this may be questioned, a weakness not only suffered by the fluid type approach adopted here.

ACKNOWLEDGMENTS

The authors wish to express gratitude for many useful discussions with R. Koch, Y. Kazakov, T. Wauters, L. Colas, S. Heuraux, L.-F. Lu, and J. Jacquot. This work has been carried out within the framework of the EUROfusion Consortium and has received funding from the Euratom research and training programme 2014-2018 under Grant Agreement No. 633053. The views and opinions expressed herein do not necessarily reflect those of the European Commission.

APPENDIX A: KLIMA'S SLOW TIME SCALE EQUATION OF MOTION

Klima derived expressions for the slow scale equation of motion for charged particles in the presence of a confining magnetic field and when a driven high frequency electromagnetic field perturbs the motion.[7] The starting point is the single particle equation of motion under the influence of the Lorentz force. Following the splitting described in the main text, one finds Eq. (4) where

$$\Theta = \frac{1}{4} Re\left[\vec{v}_1 . \vec{v}_1^{\,*} + \frac{i\vec{\Omega}}{\omega} . \vec{v}_1 \times \vec{v}_1^{\,*}\right], \tag{A1}$$

in which $\vec{\Omega} = q\vec{B}_o/m$. Introducing the notation $\vec{\epsilon} = q\vec{E}_1/m$, Θ can be written in terms of $\vec{E}_1$ to yield Eq. (5). To obtain this result, the expression

$$\vec{v}_1 = \frac{1}{\Omega^2 - \omega^2}\left[-i\omega\vec{\epsilon} + \vec{\epsilon}\times\vec{\Omega} + \frac{i\vec{\Omega}.\vec{\epsilon}}{\omega}\vec{\Omega}\right] \tag{A2}$$

is useful; the latter is found starting from the driven equation of motion, evaluating $\vec{v}_1.\vec{\epsilon}$ and $\vec{v}_1\times\vec{\epsilon}$, and combining the 2 to isolate $\vec{v}_1$. With the obtained expressions and simplifications, the equation of motion is now compactly written as

$$\frac{d\vec{v}_o}{dt} = -\frac{q\nabla\Phi}{m} - \nabla\Theta + \Omega\vec{v}_o\times\vec{e}_{//}, \tag{A3}$$

in which the notation $\vec{E}_o = -\nabla\Phi$ was introduced to reflect the fact that Faraday's law requires the electric field $\vec{E}_o$ to be the gradient of a function when $\partial/\partial t = 0$.

Subsequently, Klima extends the result found for single particles to the case of a flow adopting the assumption that the pressure is of order δ^2. Starting from an equation of motion which looks exactly like the single particle expression except for the pressure term $-N^{-1}\nabla P$ (in which N is the density and P is the pressure) and a collision term, and introducing the relevant upgraded flow velocity $\vec{V}_{o,new} = \vec{V}_o - \frac{1}{2\omega}Re[i\vec{V}_1^*.\nabla\vec{V}_1]$ to capture the net effect of the driven motion the equation can—up to δ^3 corrections—be recast in the same form as before after some manipulations. Here, $\vec{V}_o$ and $\vec{V}_1$ are the zero order and the perturbed, driven fluid velocities, respectively; capital letters were introduced by Klima to avoid confusion with the corresponding single particle quantities. Whereas the first term of the new velocity constitutes an average over a driver period at a fixed location, the second accounts for the fact that the relevant volume is itself oscillating as a function of time, i.e., the averaging is done in terms of *Lagrangian* coordinates accounting for the perturbed $\vec{E}$-field driven change of the zero order motion. Evaluating this correction requires including the leading order spatial inhomogeneity corrections to the perturbed motion adopting the same philosophy as for obtaining the Ponderomotive acceleration, while making use of Eq. (3) to link the driven acceleration, velocity, and displacement corrections. Up to higher order corrections, grouping the terms of the upgraded velocity in the right hand side of the equation, Klima formally finds the same result as before except that the zero and first order velocities are now the relevant *flow* velocities and there is the extra pressure contribution $-N_o^{-1}\nabla P = -N_o^{-1}\nabla kTN_o$. The adopted ordering and philosophy allow Klima to fold the non-linear term $Re[i\vec{V}_1^*.\nabla\vec{V}_1]/(2\omega)$ into the reference flow velocity and get a simple intuitive equation governing the zero order flow. The term in question is associated with the Reynolds stress caused by the forced oscillation. The "relevant" slow time scale fluid flow $\vec{V}_{o,new}$ is not taken to be the zero order flow velocity $\vec{V}_o$ itself but the velocity including the net correction brought about by the driven motion. This makes that—for the adopted ordering—there are 2 terms in the equation of motion that get a different role depending on the adopted dependent variable. In Klima's final expression, they are absorbed in $\vec{V}_{o,new}$. When adopting $\vec{V}_o$ as the independent variable, they constitute accelerations contributing to the modification of the flow. Either choice of variable can be made; only the interpretation of the flow is different. Klima's choice is adopted in the work presented here. It is similar in philosophy to the one made by Mc Vey *et al.*[44] and Vaclavik and Appert[45] in kinetic wave modeling of radio frequency heating and more in particular in the context of defining the kinetic flux associated with an electromagnetic wave when making a distinction between actual wave induced heating (the change of the energy in a reference volume flowing along with the wave-unperturbed motion) on the one hand, and a local change of energy due to the fact that a different number of particles stream into than out of a frozen reference volume on the other. The latter is not interpreted as "heating." Similarly but more involved, to avoid a spurious parallel acceleration term, Balescu[46] upgraded the averaging method and generalized the parallel velocity when writing down the equation of motion for the guiding center in presence of a fast perturbation. Like for the attitude taken with respect to the inclusion of kinetic effects, the assessment of the role of the term $Re[\vec{V}_1^*.\nabla\vec{V}_1]/(2\omega)$ is sidestepped at this stage. This is not equivalent to stating that the term is without importance: The wave induced stress is, e.g., seen as a key ingredient to help explain plasma rotation induced by the ion Bernstein wave (a mode requiring a kinetic description) as is discussed by Myra and D'Ippolito.[47] To lighten the notation, $\vec{V}_{o,new}$ will henceforth simply be denoted by the earlier introduced symbol for the slow time scale velocity $\vec{v}_o$, and likewise for the perturbed velocity. The collision terms introduced by Klima are omitted in the present work. Assuming the temperature T is constant one then immediately finds the generalized equation of motion Eq. (6).

APPENDIX B: INTEGRATING THE EQUATION OF MOTION: FULL AND AVERAGE DYNAMICS

Solving the equation of motion can be done as an initial value problem (in which case not only the equation for the velocity but also that for the position needs to be solved) or as a boundary value problem (in which case the time derivative is local and the solution is convected by the convection term). Two examples of the resolution of the equation of motion Eq. (6) as an initial value problem are depicted in Figs. 12 and 13, the former being an example for the ions and illustrating the force balance, the latter showing the velocities for electrons having velocities equal to 10% of the electron thermal velocity. In spite of being an equation for the "slow" time scale and as earlier demonstrated when integrating the equation by hand, the solutions have a fast (cyclotron revolution) variation, imposed by the strong magnetic field superposed on a steady drift velocity. The actual slow dynamics is then governed by

$$\frac{d\vec{x}_\perp}{dt} = \vec{v}_{drift,\perp}, \tag{B1}$$

$$\frac{d^2x_{//}}{dt^2} = \frac{dv_{//}}{dt} = a_{//}. \tag{B2}$$

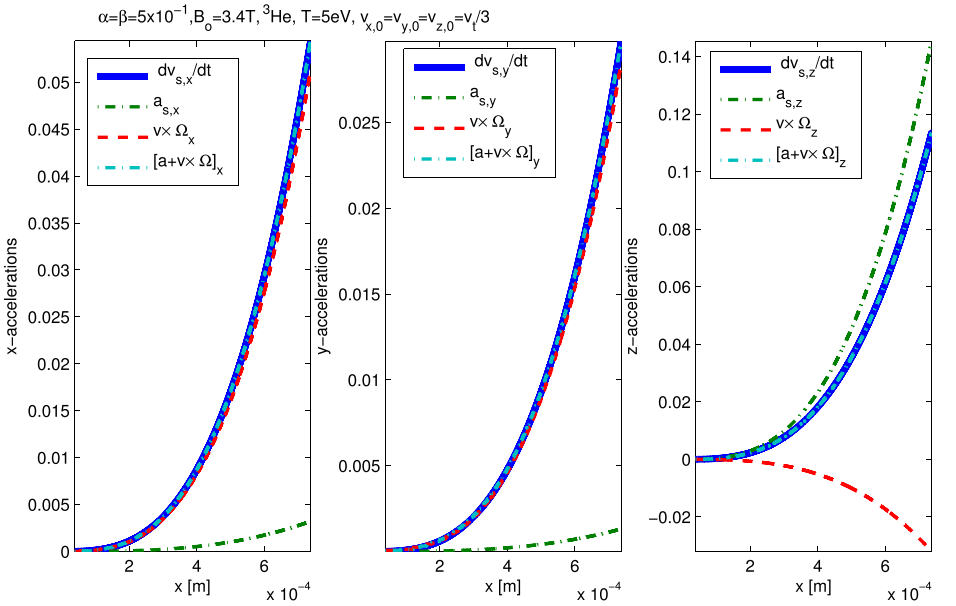

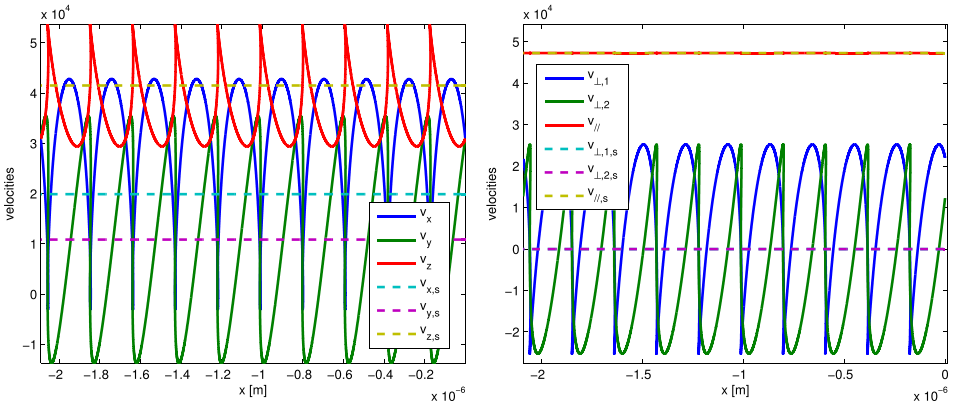

FIG. 12. Solution of the slow time scale equation of motion for ^3He ions; for this toy problem test $\vec{a}$ is assumed to be the gradient of a potential $\psi = 10^6(2x^4 + 5y^4 + 10z^4)[(\mathrm{m/s})^2]$; $\alpha = \beta = 0.5$ rad.

FIG. 13. Electron total as well as slow time scale (drift) velocities obtained solving Eq. (A3) or Eq. (B1); the magnetic field magnitude and direction is as in the previous example.

The corresponding velocities are equally depicted in the Figs. 12 and 13 for a problem with an analytically prescribed potential and constitute the average motion around which the oscillatory motion occurs. In the presence of a strong confining magnetic field, the cyclotron gyration is a typical feature of the motion adopting the particle approach; convecting the solution (i.e., solving the equation of motion for the whole region of interest at once, making use of the fact that the total derivative is composed of a partial time derivative as well as a position shift brought about by the velocity and involving the local spatial gradient) mixes the gyro-phases and modifies the role of the Lorentz term. It substitutes the fast variation by its average effect at the guiding center level: the setting up of a perpendicular drift.

[1]D. Van Eester, K. Crombé, and V. Kyrytsya, Plasma Phys. Controlled Fusion **55**, 025002 (2013).
[2]D. Van Eester, K. Crombé, and V. Kyrytsya, Plasma Phys. Controlled Fusion **55**, 055001 (2013).
[3]M. Dirickx, "Contribution à l' étude du transport néo-classique dans un plasma de tokamak en présence d'un champ électrique intense et/ou à variation spatiale rapide," Ph.D. thesis, Université Libre de Bruxelles and Report LPP-ERM/KMS No. 117, 1999.
[4]V. S. Chan and S. C. Chiu, Phys. Fluids **22**, 1724 (1979).
[5]O. Meneghini, "Full wave modeling of lower hybrid waves on Alcator C-Mod," Ph.D. thesis, MIT, Boston, USA, 823507517, 2012.
[6]O. Meneghini, S. Shiraiwa, C. Lau, I. Faust, B. La Bombard, G. Wallace, R. Parker, R. Wilson, S. Wukitch, and the Alcator C-Mod team, "Modeling non-linear plasma-wave interaction at the edge of a tokamak plasma," COMSOL Conference, Boston, USA, 2011.
[7]R. Klima, Czech. J. Phys. **B 18**, 1280 (1968).
[8]W. Zhang, V. Bobkov, T. Lunt, J.-M. Noterdaeme, D. Coster, R. Bilato, P. Jacquet, D. Brida, Y. Feng, E. Wolfrum, L. Guimarais, and the ASDEX Upgrade Team, "3D simulations of gas puff effects on edge density and ICRF coupling in ASDEX upgrade," Nucl. Fusion (submitted).
[9]R. Ochoukov, D. G. Whyte, D. Brunner, D. A. D'Ippolito, B. La Bombard, B. Lipschultz, J. R. Myra, J. L. Terry, and S. J. Wukitch, Plasma Phys. Controlled Fusion **56**(1), 015004 (2014).
[10]J. R. Myra, L. A. Berry, D. A. D'Ippolito, and E. F. Jaeger, Phys. Plasmas **11**, 1786 (2004).
[11]J. R. Myra, D. A. D'Ippolito, D. A. Russell, L. A. Berry, E. F. Jaeger, and M. D. Carter, Nucl. Fusion **46**, S455 (2006).
[12]Z. Gao, N. J. Fisch, H. Qin, and J. R. Myra, Phys. Plasmas **14**, 084502 (2007).
[13]J. Chen and Z. Gao, Phys. Plasmas **20**, 082508 (2013).
[14]C. C. Hegna and J. D. Callen, Phys. Plasmas **16**, 112501 (2009).
[15]S. Devaux and G. Manfredi, Phys. Plasmas **13**, 083504 (2006).
[16]S. Devaux and G. Manfredi, Plasma Phys. Controlled Fusion **50**, 025009 (2008).
[17]F. Valsaque and G. Manfredi, J. Nucl. Mater. **290–293**, 763–767 (2001).
[18]R. Chodura, Phys. Fluids **25**(9), 1628 (1982).
[19]G. Manfredi, S. Hirstoaga, and S. Devaux, Plasma Phys. Controlled Fusion **53**, 015012 (2011).
[20]E. F. Jaeger, R. W. Harvey, L. A. Berry, J. R. Myra, R. J. Dumont, C. K. Phillips, D. N. Smithe, R. F. Barrett, D. B. Batchelor, P. T. Bonoli, M. D. Carter, E. F. D'Azevedo, D. A. D'Ippolito, R. D. Moore, and J. C. Wright, Nucl. Fusion **46**, S397 (2006).

[21]D. Smithe, Phys. Plasmas **14**, 056104 (2007).
[22]T. G. Jenkins, T. M. Austin, D. N. Smithe, J. Loverich, and A. H. Hakim, Phys. Plasmas **20**, 012116 (2013).
[23]D. G. Swanson, *Plasma Waves* (Academic Press, New York, 1989).
[24]F. Louche, in *Proceedings of 7th European Fusion Theory Conference*, 1997, Vol. 1, p. 287.
[25]J. D. Callen, *Fundamentals of Plasma Physics* (University of Wisconsin, Madison, 2003).
[26]A. Boschi and F. Agistrelli, Il Nuovo Cimento **XXIX**(2), 55 (1963).
[27]M. Abramowitz and I. A. Stegun, *Handbook of Mathematical Functions with Formulas, Graphs, and Mathematical Tables* (Dover Publications, New York, 1964).
[28]T. H. Stix, *Waves in Plasmas* (Springer-Verlag, New York, 1992).
[29]P. C. Stangeby, *The Plasma Boundary of Magnetic Fusion Devices*, Plasma Physics Series (IOP, Bristol and Philadelphia, 2000).
[30]T. Wauters, A. Lyssoivan, D. Douai, O. Marchuk, D. Wünderlich, R. Koch, G. Sergienko, G. Van Oost, and M. Van Schoor, Plasma Phys. Controlled Fusion **53**, 125003 (2011).
[31]T. Wauters, "Study and optimization of magnetized ICRF discharges for tokamak wall conditioning and assessment of the applicability to ITER," Ph.D. thesis, Ghent University and Royal Military Academy, 2011.
[32]A. Fukuyama, S.-I. Itoh, and K. Itoh, J. Phys. Soc. Jpn. **51**, 1010 (1982).
[33]D. Van Eester, K. Crombé, and Y. Kazakov, "Kinetic description of wave induced plasma flow in the radio frequency domain," e-print arXiv:1403.4770 (physics.plasm-ph).
[34]B. Van Compernolle, R. Maggiora, G. Vecchi, D. Milanesio, and R. Koch, in *Proceedings of 35th EPS Conference on Plasma Physics*, 2008, Vol. ECA 32D, P-2.105.
[35]J. Myra, D. A. D'Ippolito, and M. J. Gerver, Nucl. Fusion **30**, 845 (1990).
[36]J. R. Myra, D. A. D'Ippolito, and M. Bures, Phys. Plasmas **1**, 2890 (1994).
[37]D. A. D'Ippolito, J. R. Myra, J. H. Rogers, K. W. Hill, J. C. Hosea, R. Majeski, G. Schilling, J. R. Wilson, G. R. Hanson, A. C. England, and J. B. Wilgen, Nucl. Fusion **38**, 1543 (1998).
[38]D. A. D'Ippolito and J. R. Myra, Phys. Plasmas **13**, 102508 (2006).
[39]D. A. D'Ippolito, J. R. Myra, E. F. Jaeger, and L. A. Berry, Phys. Plasmas **15**, 102501 (2008).
[40]D. A. D'Ippolito and J. R. Myra, Phys. Plasmas **16**, 022506 (2009).
[41]D. A. D'Ippolito and J. R. Myra, Phys. Plasmas **17**, 072508 (2010).
[42]D. A. D'Ippolito and J. R. Myra, J. Nucl. Mater. **415**, S1001 (2011).
[43]D. A. D'Ippolito and J. R. Myra, Phys. Plasmas **19**, 034504 (2012).
[44]B. D. McVey, R. S. Sund, and J. E. Scharer, Phys. Rev. Lett. **55**, 507 (1985).
[45]J. Vaclavik and K. Appert, Plasma Phys. Controlled Fusion **29**, 257 (1987).
[46]R. Balescu, *Transport Processes in Plasmas* (Elsevier Science Publishers, Amsterdam, 1988), Vols. 1 and 2.
[47]J. R. Myra and D. A. D'Ippolito, AIP Conf. Proc. **485**, 391 (1999).